HHS Public Access

Author manuscript

Sci Transl Med. Author manuscript; available in PMC 2021 June 02.

Published in final edited form as:

Sci Transl Med. 2020 December 02; 12(572): . doi:10.1126/scitranslmed.aaz2841.

Glycine-based treatment ameliorates NAFLD by modulating fatty acid oxidation, glutathione synthesis, and the gut microbiome

Oren Rom[1,*], **Yuhao Liu**[1], **Zhipeng Liu**[2], **Ying Zhao**[1], **Jianfeng Wu**[3], **Alia Ghrayeb**[4], **Luis Villacorta**[1], **Yanbo Fan**[5], **Lin Chang**[1], **Lu Wang**[6], **Cai Liu**[6], **Dongshan Yang**[7], **Jun Song**[7], **Jason C. Rech**[8], **Yanhong Guo**[1], **Huilun Wang**[1], **Guizhen Zhao**[1], **Wenying Liang**[1], **Yui Koike**[1], **Haocheng Lu**[1], **Tomonari Koike**[1], **Tony Hayek**[9,10], **Subramaniam Pennathur**[1], **Chuanwu Xi**[3], **Bo Wen**[6], **Duxin Sun**[6], **Minerva T. Garcia-Barrio**[1], **Michael Aviram**[9], **Eyal Gottlieb**[4], **Inbal Mor**[4], **Wanqing Liu**[11], **Jifeng Zhang**[1], **Y. Eugene Chen**[1,7,*]

[1]Department of Internal Medicine, University of Michigan, Ann Arbor, MI 48109, USA.

[2]Department of Medicinal Chemistry and Molecular Pharmacology, Purdue University, West Lafayette, IN 47907, USA.

[3]Department of Environmental Health Sciences, University of Michigan School of Public Health, Ann Arbor, MI 48109, USA.

[4]The Cancer Metabolism Laboratory, the Ruth and Bruce Rappaport Faculty of Medicine, Technion-Israel Institute of Technology, Haifa 31096, Israel.

[5]Department of Cancer Biology and Department of Internal Medicine, Division of Cardiovascular Health and Disease, University of Cincinnati College of Medicine, Cincinnati, OH 45267, USA.

[6]Department of Pharmaceutical Sciences, College of Pharmacy, University of Michigan, Ann Arbor, MI 48109, USA.

[7]Center for Advanced Models for Translational Sciences and Therapeutics, University of Michigan Medical Center, Ann Arbor, MI 48109, USA.

[8]Michigan Center for Therapeutic Innovation, University of Michigan, Ann Arbor 48109, MI, USA.

[9]The Lipid Research Laboratory, Rappaport Faculty of Medicine, Technion-Israel Institute of Technology, Haifa 31096, Israel.

[*]To whom correspondence should be addressed: echenum@umich.edu (Y.E.C.); roren@umich.edu (O.R.).

Author contributions: O.R., J.Z. and Y.E.C. conceived and designed the study. O.R., Y.L., Z.L., Y.Z., J.W., A.G., L.V., L.W., C.L., Y.G., H.W., B.W., I.R. and W.L. contributed to data acquisition and/or analysis. Y.F., L.C., D.Y., J.S., J.C.R., G.Z., W.L., Y.K., H.L., T.K., S.P., E.G., C.X. and D.S. provided technical or material support. O.R., Z.L., J.W. and W.L. performed statistical analyses. O.R., Z.L. and J.W wrote the manuscript. L.V., Y.F., L.C., T.H., S.P., M.T.G-B., M.A., E.G., I.M., W.L., J.Z. and Y.E.C contributed to the discussion and important intellectual content. Y.E.C. and O.R directed and supervised the study.

Competing interests: O.R., Y.Z., J.Z. and Y.E.C. have filed a patent application based on this work (Tri-peptides and treatment of metabolic, cardiovascular and inflammatory disorders, PCT/US2019/046052). Y.E.C. is the founder of Diapin Therapeutics, which provided DT-109/110 for this study. All other authors declare that they have no competing interests.

Data and materials availability: All data associated with this study are in the main paper or supplementary materials. RNA-sequencing data have been deposited in NCBI's SRA (accession number: PRJNA556537) or GEO (accession number: GSE126204). Metagenomics sequencing data have been deposited in NCBI's SRA (accession number: PRJNA544728).

Supplementary Materials:
Materials and Methods
Data File S1. Raw data.
References (61–75)

[10]Department of Internal Medicine E, Rambam Health Care Campus, Haifa 31096, Israel.

[11]Department of Pharmaceutical Sciences and Department of Pharmacology, Wayne State University, Detroit, MI 48201, USA.

Abstract

Nonalcoholic fatty liver disease (NAFLD) including nonalcoholic steatohepatitis (NASH) has reached epidemic proportions with no pharmacological therapy approved. Lower circulating glycine is consistently reported in patients with NAFLD, but the causes for reduced glycine, its role as a causative factor, and its therapeutic potential remain unclear. We performed transcriptomics in livers from humans and mice with NAFLD and found suppression of glycine biosynthetic genes, primarily alanine-glyoxylate aminotransferase 1 (*AGXT1*). Genetic (*Agxt1*$^{-/-}$ mice) and dietary approaches to limit glycine availability resulted in exacerbated diet-induced hyperlipidemia and steatohepatitis, with suppressed mitochondrial/peroxisomal fatty acid β-oxidation (FAO) and enhanced inflammation as the underlying pathways. We explored glycine-based compounds with dual lipid/glucose-lowering properties as potential therapies for NAFLD, and identified a tripeptide (Gly-Gly-L-Leu, DT-109) that improved body composition and lowered circulating glucose, lipids, transaminases, pro-inflammatory cytokines and steatohepatitis in mice with established NASH induced by a high-fat, cholesterol, and fructose diet. We applied metagenomics, transcriptomics and metabolomics to explore the underlying mechanisms. The bacterial genus *Clostridium sensu stricto* was markedly increased in mice with NASH and decreased following DT-109 treatment. DT-109 induced hepatic FAO pathways, lowered lipotoxicity, and stimulated *de novo* glutathione synthesis. In turn, inflammatory infiltration and hepatic fibrosis were attenuated via suppression of nuclear factor-kappa B (NFκB) target genes and transforming growth factor-beta (TGFβ)/SMAD signaling. Unlike its effects on the gut microbiome, DT-109 stimulated FAO and glutathione synthesis independent of NASH. In conclusion, impaired glycine metabolism may play a causative role in NAFLD. Glycine-based treatment attenuates experimental NAFLD by stimulating hepatic FAO and glutathione synthesis, thus warranting clinical evaluation.

One Sentence Summary:

A glycine-related compound improves symptoms in a mouse model of NAFLD, a disease that is currently without approved treatments.

Introduction

Nonalcoholic fatty liver disease (NAFLD), the most common chronic liver disease, affects 25% of the population worldwide (1). NAFLD encompasses a spectrum of liver pathologies ranging from simple hepatic steatosis (HS), nonalcoholic steatohepatitis (NASH) characterized by hepatocyte damage and lobular inflammation in association with fibrosis progression, and cirrhosis that may lead to liver failure or hepatocellular carcinoma (2, 3). Cardiometabolic comorbidities including obesity, type 2 diabetes (T2D), metabolic syndrome (MetS), and dyslipidemia are common in NAFLD (1). Apart from liver-specific mortality, cardiovascular disease is a leading cause of death in patients with NAFLD,

particularly those with NASH (1, 2, 4). Despite the global burden of NAFLD and substantial efforts in drug development, no therapy has been approved so far (5).

Considerable advances, particularly in metabolomics and the gut microbiome, have improved our understanding of NAFLD pathogenesis, suggesting new therapeutic targets (5). Whereas abnormal lipid and carbohydrate metabolism are known features of NAFLD (6), recent metabolomics-based studies indicate that dysregulated metabolism of specific amino acids plays a role in NAFLD pathogenesis. Particularly, whereas most circulating amino acids are increased in NAFLD, glycine concentrations are decreased (7) and are negatively correlated with HS (8), hepatocyte ballooning, and lobular inflammation (9). Lower plasma glycine together with known biomarkers (for example aspartate-aminotransferase, AST, and patatin-like phospholipase domain containing-3 [*PNPLA3*] genotype) was recently included in a model to predict NASH (10). Furthermore, lower circulating glycine is associated with higher prevalence of NAFLD comorbidities including obesity (11), T2D (12), MetS (13), coronary heart disease, and myocardial infarction (14, 15), whereas higher glycine concentrations are associated with a favorable lipid profile (14).

The non-essential amino acid glycine is synthesized from several precursors mainly in the liver. These reactions are catalyzed by key enzymes driving glycine formation from serine (serine hydroxymethyltransferases, SHMTs), threonine (threonine dehydrogenase, TDH), choline via sarcosine (choline dehydrogenase, CHDH; sarcosine dehydrogenase, SARDH) and from alanine to glyoxylate (AGXTs) (16). Glycine is used in multiple pathways to generate essential molecules including purines, glutathione (GSH), heme, and creatine (16). In line with epidemiological evidences linking lower circulating glycine to cardiometabolic diseases, studies in humans (17, 18) or in rodent models (19–24) reported glucose/lipid-lowering, hepatoprotective, or anti-inflammatory effects in response to glycine administration. Nevertheless, a comprehensive investigation of the roles of glycine in NAFLD, applying models that fully mimic the human disease and accurate dosing, has not been pursued.

Considering the burden of NAFLD, lack of available therapies, and consistent reports associating lower circulating glycine to NAFLD severity, there is a strong rationale to better understand glycine metabolism in NAFLD, which could lead to novel therapeutics. In the current study, we aimed to investigate whether altered glycine metabolism contributes to NAFLD development by performing transcriptomics in livers from humans and mice with NAFLD and through genetic and dietary approaches to limit glycine availability in mice. We further explored glycine-based compounds as potential therapies for NAFLD and their mechanisms of action.

Results

Impaired glycine biosynthesis in human and murine NAFLD

To test whether altered glycine metabolism contributes to NAFLD development, we first studied C57BL/6J mice with Western-diet (WD)-induced HS. After 12 weeks on WD, hypercholesterolemia (Fig. 1A) and HS, verified by H&E and Oil Red O (ORO) staining, quantification of hepatic triglycerides (TG), and total cholesterol (TC) were evident (Fig.

1B–D). Targeted metabolomics revealed that among all amino acids, plasma glycine was most significantly reduced (P=0.0111), whereas its precursors serine, threonine, and alanine were increased (Fig. 1E), indicating impaired glycine biosynthesis. Accordingly, key glycine biosynthetic genes were downregulated in livers from mice with HS, among which *Agxt1* was most significantly suppressed (P=0.0002, Fig. 1F). Additionally, *AGXT1* was markedly downregulated in HepG2 cells upon palmitic acid (PA)-induced TG accumulation (Fig. 1 G, H).

To assess whether a similar pattern was evident in more severe NAFLD, we performed RNA-sequencing of livers from mice with advanced NASH and fibrosis induced by 24 weeks on high-fat, high-cholesterol, high-fructose NASH-diet (25) (Fig. 1I, Fig. S1A). Pathway analysis revealed alternations in known pathways implicated in NASH, including upregulation of chemokines, NF-κB, toll-like receptor (TLR), and TGFβ signaling, along with downregulation of fatty acid degradation and peroxisome proliferator-activated receptor (PPAR) signaling (Fig. S1B). Pathways regulating amino acid biosynthesis, particularly metabolism of glycine, serine, threonine, and glyoxylate were suppressed in NASH (Fig. S1B), including downregulation of *Agxt1* (P=0.0009, Fig. 1J). Using an independent cohort of mice with diet-induced NASH, we confirmed *Agxt1* suppression by qPCR (Fig. 1K).

To address whether glycine biosynthetic genes are similarly suppressed in humans with advanced NAFLD, we performed a meta-analysis based on transcriptomics of livers from patients with NASH (26, 27). We found that *AGXT1* (beta=−0.141, P=0.0041) and *AGXT2* (beta=−0.134, P=0.0135) were significantly downregulated in NASH, whereas D-amino acid oxidase (*DAO*), which catalyzes glycine degradation to glyoxylate, was upregulated (beta=0.216, P=0.0025, Fig. 1L). Among 206 samples obtained from liver transplantation donors (28), we found that *AGXT1* expression inversely correlated with hepatic fat content (r=−0.196, P=0.0049, Fig. 1M). A similar inverse correlation was found between the expression of *PPARA*, a master regulator of hepatic FAO (2, 29), and hepatic fat content (r=−0.154, P=0.0275, Fig. S2A), whereas expression of C-C motif chemokine ligand 5 (*CCL5*) and *TGFB*, key players in steatohepatitis and fibrosis (2, 30), positively correlated with hepatic fat (r=0.185, P=0.0078 and r=0.284, P<0.0001, respectively, Fig. S2B, C). Thus, in line with recent reports of lower circulating glycine in NAFLD (7–9), we found suppression of glycine biosynthetic genes, predominantly *AGXT1*, a liver-specific gene localized to the peroxisome or mitochondria of hepatocytes (31, 32).

Loss of AGXT1 exacerbates diet-induced hyperlipidemia and NASH

To study a potential role of AGXT1 in HS, we first knocked down *AGXT1* in HepG2 cells using siRNA, which enhanced PA-induced TG accumulation (Fig. 2A–C). In contrast, AGXT1 overexpression decreased cellular TGs (Fig. 2D, E). To study the effects of loss of *AGXT1 in vivo*, we generated $Agxt1^{-/-}$ mice using CRISPR/Cas9 (Fig. 2F). Western blot confirmed the absence of AGXT1 in livers from $Agxt1^{-/-}$ mice (Fig. 2G), and the lower plasma ratio of glycine to oxalate confirmed impaired enzymatic activity (Fig. 2H). On standard chow-diet (CD), liver histology of $Agxt1^{-/-}$ mice was comparable to that of $Agxt1^{+/+}$ as previously indicated (33), and we additionally found that plasma liver enzymes and hepatic expression of genes regulating FAO, inflammation, or fibrosis were also

comparable (Fig. S3A–G). However, after 12 weeks on NASH-diet, *Agxt1*$^{-/-}$ mice had increased plasma TGs, TC, AST and ALT (Fig. 2I–L). Gross appearance of the peritoneal cavities revealed larger livers with enhanced yellowish coloration in *Agxt1*$^{-/-}$ mice (Fig. 3A). Although no significant differences were noted in body weight, liver weight was increased (Fig. 3B, Fig. S4A, B) and associated with enhanced HS and fibrosis in *Agxt1*$^{-/-}$ mice (Fig. 3A, C, D). Histological analyses based on H&E and Sirius Red staining confirmed higher NAFLD activity score (NAS) and fibrosis score in *Agxt1*$^{-/-}$ mice (Fig. 3E, F, Fig. S4C).

To understand the underlying mechanisms of accelerated diet-induced NASH in *Agxt*$^{-/-}$ mice, we performed RNA-sequencing of livers from *Agxt1*$^{+/+}$ and *Agxt1*$^{-/-}$ mice followed by qPCR validation. Pathway analysis revealed suppression of energy metabolism and FAO pathways in *Agxt1*$^{-/-}$ mice, and upregulation of pro-inflammatory pathways (Fig. 3G, Fig. S4D). Genes regulating peroxisomal (acyl-CoA thioesterase-3 [*Acot3*], acyl-CoA synthetase mediumchain-5 [*Acsm5*], acyl-CoA synthetase long-chain-1 [*Acsl1*]) and mitochondrial FAO (hydroxyacyl-CoA dehydrogenase-alpha/beta [*Hadha*/*Hadhb*] and acetyl-CoA acyltransferase-2 [*Acaa2*]) were downregulated in *Agxt1*$^{-/-}$ mice (Fig. 3H–J, with a similar trend for *Ppara*, P=0.0557), whereas genes encoding for regulators of pro-inflammatory signaling (*Nfkb1*/*Nfkb2*, *Relb*, *Ccr2*/*Ccr5*, and *Tlr2*/*Tlr4*), cytokines (tumor necrosis factor [*Tnf*] and *Ccl2*), fibrogenesis (*Tgfb1*/*Tgfb2* and *Tgfbr2*) and extracellular matrix (ECM) remodeling (collagen, type-I, alpha-2 [*Col1a2, Col4a2*] and tissue inhibitor of metalloproteinase 1 [*Timp1*]) were upregulated (Fig. 3H,K,L). Thus, AGXT1, a liver-specific glycine biosynthetic enzyme, is suppressed in NAFLD, and its deficiency accelerates diet-induced NASH.

Glycine deficiency exacerbates diet-induced hyperlipidemia, hyperglycemia, and hepatic steatosis

Lower circulating glycine is associated with NAFLD (7–9), T2D and cardiometabolic diseases (11–15), whereas higher plasma glycine concentrations are associated with a favorable lipid profile (14) (Table S1). To investigate a role of dietary glycine in dyslipidemia in relation to HS, we developed amino acid-modified WD with or without glycine (WD_{AA}+Gly or WD_{AA}−Gly, Table S2) and fed *Apoe*$^{-/-}$ mice CD, WD_{AA}+Gly or WD_{AA}−Gly for 10 weeks. On WD, *Apo*$^{-/-}$ mice not only present severe dyslipidemia, but also abnormal glucose tolerance and HS (25, 34), allowing the study of dietary glycine in dyslipidemia, hyperglycemia, and HS simultaneously. We found significant decrease in plasma glycine in mice fed WD_{AA}−Gly (P=0.0015, Fig. S5A). Nuclear magnetic resonance (NMR)-based body composition and comprehensive laboratory animal monitoring system (CLAMS) analyses indicated increased body weight and fat in mice fed WD_{AA}−Gly, but not in mice fed WD_{AA}+Gly (Fig. S5B–D). Food intake and respiratory exchange ratio (RER) were similarly decreased in mice fed WD_{AA}+Gly and WD_{AA}−Gly, with no significant changes in total activity and energy expenditure (Fig. S5E–H). Accordingly, plasma leptin was increased in mice fed WD_{AA}−Gly (Fig. S5I) and increased adipocyte hypertrophy was noted in epididymal and subcutaneous adipose tissues (EAT and SAT, Fig. S5J). Compared to WD_{AA}+Gly, mice fed WD_{AA}−Gly had increased plasma TC and TG (Fig. S6A–D). Increased plasma glucose was noted in mice fed WD_{AA}−Gly, but not in mice fed WD_{AA}

+Gly (Fig. S6E). Histology and lipid quantification revealed increased HS following WD_{AA} −Gly feeding (Fig. S6F–H). Linear regression analyses indicated inverse correlations between plasma glycine concentrations and plasma TC, glucose or liver TG (Fig. S6I–K). Thus, dietary glycine deficiency exacerbates hyperlipidemia, hyperglycemia and HS in hyperlipidemic mice.

DT-109: a glycine-based tripeptide with dual glucose/lipid-lowering properties

Considering our findings above together with a large body of evidence linking lower circulating glycine with dyslipidemia as well as with prediabetes and T2D (12–14), we reasoned that glycine-based compounds may have a therapeutic potential through a dual glucose/lipid-lowering effect. Thus, we searched for compounds structurally similar to glycine and selected 10 compounds representing structural, conformational, electrostatic or isosteric modifications to the glycine scaffold (Fig. S7A–K), four of which were suitable for oral administration (median lethal dose [LD_{50}]>1 mg/g). Chronic glycine supplementation (1 mg/g/day) was found to reduce circulating TG in *Apoe*$^{-/-}$ mice (19), restore glucose tolerance and accelerate fat loss in obese C57BL/6 mice (20). In humans, ingestion of glycine together with glucose attenuated the increase in plasma glucose by >50% (17). To test glucose-lowering effects, we performed oral glucose tolerance tests (OGTT) in C57BL/6J mice administered glycine or glycine-based compounds (0.5 mg/g). None of the tested compounds attenuated the increase in blood glucose more efficiently than glycine (Fig. S8A–D). Another amino acid reported to lower glucose in mice is leucine (35). Previous studies from our lab revealed profound glucose-lowering effects for DT-109, a tripeptide of glycine combined with leucine (Gly-Gly-L-Leu) (36). We tested DT-109 or its D-isomer (Gly-Gly-D-Leu, DT-110) in OGTT. Whereas the glucose-lowering effects of DT-110 were similar to glycine, DT-109 was the only compound that lowered glucose more efficiently than glycine (Fig. S8E, F), particularly when compared to equivalent amounts of its individual amino acids (Fig. S8G). In parallel with the robust reduction in hyperglycemia, peak plasma DT-109 was previously reported after 30 min from oral administration (36). In line, peak liver DT-109 was found after 30 min from oral administration (Fig. S8H).

To test the effects of DT-109 on dyslipidemia, hyperglycemia, and HS simultaneously, we fed *Apo*$^{-/-}$ mice WD with oral administration of 1 mg/g/day DT-109 (36) or equivalent amounts of leucine, glycine, or H_2O (Fig. S9A). After 10 weeks, DT-109 had the most potent glucose-lowering effects both in OGTT and in non-fasting glucose (Fig. S9B, C). No significant differences in food intake or body weight were observed (Fig. S9D, E). Lipid profile analyses showed that mice treated with DT-109 had the lowest TC and LDL, without the reduction in HDL noted in glycine-treated mice or significant differences in plasma TG (Fig. S9F–J). Glycine or DT-109 reduced leptin and adipocyte hypertrophy in EAT and SAT (Fig. S9K, L). Furthermore, gross appearance of the peritoneal cavities and histological analyses revealed reduced HS in livers from mice treated with glycine or DT-109, but not with leucine (Fig. S10A). qPCR analyses revealed upregulation of key genes regulating FAO in livers from mice treated with glycine or DT-109 (*Ppara*, *Pnpla2*, carnitine/acylcarnitine translocase [*Cact*], carnitine palmitoyltransferase 1a [*Cpt1a*], and acyl-CoA dehydrogenase-long chain [*Acadl*]), and downregulation of *Ccl2* by glycine treatment without changes in

Tnf (Fig. S10B). Thus, DT-109 has dual glucose/lipid-lowering properties and prevents WD-induced HS in hyperlipidemic mice.

DT-109 improves body composition and protects against diet-induced NASH

To further explore the therapeutic potential of DT-109 against NASH, we devised an experimental approach to model advanced NAFLD (Fig. 4A). C57BL/6J mice fed NASH-diet for 12 weeks had increased circulating glucose, TC, AST, and ALT compared to those fed CD (Fig. S11A). A subset of the mice was sacrificed, confirming increased liver weight following NASH-diet feeding (Fig. S11B). Histological analyses revealed HS, hepatocyte ballooning, infiltration of inflammatory cells, and early fibrosis (Fig. S11C). After confirming NASH (Fig. S11D), the rest of the mice were randomized to orally receive DT-109 at 0.125 or 0.5 mg/g/day, or equivalent amounts of leucine, glycine or H_2O for 12 additional weeks on NASH-diet. Mice fed CD and administered H_2O served as control (Fig. 4A).

At week 18, OGTT and non-fasting glucose measurements confirmed a most potent glucose-lowering effect for 0.5 mg/g/day DT-109 (Fig. S11E, F). Body composition analysis revealed increased body weight in all the groups fed NASH-diet compared to CD (Fig. 4B). Compared to mice fed NASH-diet and administered H_2O, mice treated with 0.5 mg/g/day DT-109 showed reduced body fat with preserved lean mass (Fig. 4C, D) and decreased adipocyte hypertrophy in EAT and SAT, without significant differences in food intake (Fig. S12A, B). The metabolic response to diet-induced obesity involves a shift towards higher fat versus lower carbohydrate utilization, reflecting a reduction in RER (25, 37). CLAMS analysis revealed decreased RER in all groups fed NASH-diet, but no significant differences were noted in mice treated with 0.5 mg/g/day DT-109 (Fig. S12C–E). No significant differences in energy expenditure or activity were noted (Fig. S12F, G).

At endpoint, the increase in plasma AST, ALT, and alkaline phosphatase (ALP) observed in mice fed NASH-diet was attenuated by glycine or DT-109 (Fig. 4E–G). Plasma TG were decreased in mice treated with glycine or DT-109 (Fig. 4H), and TC was decreased only by 0.5 mg/g/day DT-109 (Fig. 4I). Accordingly, the severe hepatomegaly induced by NASH-diet was markedly attenuated by treatment with glycine or DT-109, but not with leucine (Fig. 4J, K, Fig. S13A), with NAS significantly decreased by 0.5 mg/g/day DT-109 (P=0.0403, Fig. 4L, Fig. S13B). Linear regression analyses indicated highly significant positive correlations between plasma AST, ALT, or ALP and individual NAS or fibrosis scores (P<0.0001, Fig. S13C–H).

The effects of DT-109 on the gut microbiome

To explore potential mechanisms by which glycine-based treatment protects against diet-induced NASH, we applied several approaches including metagenomics, transcriptomics, and metabolomics. An altered microbiome (dysbiosis) has emerged as a potential risk factor in NAFLD (2, 5). Particularly, dysbiosis of the gut microbiota has been linked with dysregulated amino acid metabolism in NAFLD pathogenesis (38). To investigate the gut microbiome response to glycine-based treatment for NASH, we analyzed the fecal microbiota both before and after 2 and 10 weeks of treatments using 16S rDNA sequencing

(Fig. 4A). Principal component analysis (PCA) and hierarchical clustering of operational taxonomic units (OTUs) revealed a distinct microbial composition in mice with NASH before treatments (Fig. S14A, B). Linear discriminant analysis (LDA) effect size (LEfSe) revealed a phylum-level shift including increased *Proteobacteria* in NASH, whereas *Actinobacteria* and *Tenericutes* were increased in CD. At the order level, *Clostridiales* was markedly overrepresented in NASH with increased abundance of the *Clostridiaceae-1* family and a significant 10-fold increase in the genus *Clostridium sensu stricto* ($P<0.0001$, Fig. S15A, B). After 2 weeks, minor differences were noted between treatment groups (Fig. S16A, B). However, after 10 weeks, the gut microbiome of mice fed NASH-diet and administered H_2O or leucine clustered together separately from glycine or DT-109 (Fig. 5A, B). *Clostridium sensu stricto* remained overrepresented in NASH, but not in treated mice, whereas *Alistipes* and *Oscillibacter* were overrepresented in CD (Fig. 5C, Fig. S17A). To identify bacteria related to NASH severity, we next evaluated the correlations between altered genera and NAFLD-related parameters. *Oscillibacter*, *Alistipes*, and *Pseudoflavonifractor* inversely correlated with NAS and liver weight, and, *Clostridium sensu stricto* showed significant positive correlations with all NAFLD-related parameters ($P<0.01$, Fig. 5D). Accordingly, during treatment with DT-109 or in CD-fed mice, the relative abundance of *Clostridium sensu stricto* was decreased (Fig. 5E), whereas that of *Alistipes* was increased (Fig. 5F). *Pseudoflavonifractor* and *Oscillibacter* were overrepresented only on CD throughout the study (Fig. S17B, C). To test whether the different microbial composition was caused directly by DT-109 treatment, we next tested the effects of DT-109 on the gut microbiome independent of NASH. C57BL/6J mice were fed the same CD and treated with DT-109 or water for 10 weeks. As found on NASH-diet, DT-109 significantly lowered non-fasting glucose, plasma TG and TC on CD ($P<0.05$, Fig. 5G–I), with no significant differences in food intake or body weight (Fig. S18A, B). PCA and LEfSe analysis indicated no significant differences in the gut microbiome at baseline (Fig. S18C, D), whereas at endpoint, the gut microbiome of mice treated with DT-109 clustered together separately from mice treated with water (Fig. 5J). Analysis of OTUs and LEfSe showed a phylum-level change of decreased *Firmicutes* and increased *Bacteroidetes* in mice treated with DT-109 (Fig. 5K, Fig. S18E, F) which was not observed on NASH-diet. Although lowering the relative abundance of *Clostridium sensu stricto* only at week 8, DT-109 had no significant effects on *Alistipes, Pseudoflavonifractor,* and *Oscillibacter* (Fig. 5L, M, Fig. S18G, H). These findings indicated that the different microbiome observed on NASH-diet is unlikely to be the result of a direct effect of DT-109 and led us to further explore the mechanisms by which glycine-based treatment protects against NASH.

DT-109 reverses NASH-diet-induced transcriptome alterations, impaired FAO, and hepatic lipotoxicity

To further explore potential mechanisms, we performed RNA-sequencing of livers collected at endpoint. PCA revealed that the gene expression profile from mice on NASH-diet treated with leucine clustered with H_2O controls, with intermediate patterns for glycine and 0.125 mg/g/day DT-109, whereas 0.5 mg/g/day DT-109 clustered closer to mice on CD (Fig. 6A). Volcano plots demonstrated major alterations in differentially expressed genes (DEG) in mice fed NASH-diet and treated with H_2O or leucine compared to CD (3606 or 3145 DEG, respectively) that were markedly reduced by treatment with glycine or DT-109 at 0.125 or

0.5 mg/g/day (1300, 1093 or 642 DEG, respectively, Fig. 6B). Analysis of the top 50 DEG further underscored the similarity of 0.5 mg/g/day DT-109 to the CD group (Fig. S19). Pathway analysis comparing the NASH-diet H_2O control to CD confirmed suppression of pathways regulating glycine biosynthesis and glyoxylate metabolism, with downregulation of *Agxt1*, *Shmt1* and *Sardh* and pathways regulating energy metabolism, FAO, and GSH metabolism. In contrast, known NASH-related pro-inflammatory/fibrotic pathways were upregulated (Fig. S20A, B). Pathway analysis comparing NASH-diet H_2O control to 0.5 mg/g/day DT-109 showed a similar pattern to CD, indicating that DT-109 reversed NASH-diet-induced alterations in underlying pathways (Fig. 6C, Fig. S21A). Analysis of genes implicated in major aspects of NASH pathogenesis (Fig. 6D), revealed that key genes regulating FAO (*Ppapra,* PPARG coactivator-1alpha [*Ppargc1a*] acyl-CoA oxidase-1 [*Acox1*], *Cpt2*, *Acads*/*Acadm*/*Acadl*, *Hadha*/*Hadhb, Acot3*/*Acot4* and enoyl-CoA delta isomerase 1 and 2 [*Eci1/2*]) were overrepresented in CD-fed mice and suppressed in mice fed NASH-diet and treated with H_2O or leucine. qPCR analyses confirmed that treatment with glycine or DT-109 significantly upregulated *Ppargc1a* and *Acot3*/*Acot4* compared to NASH-diet H_2O control, whereas *Acsl1*, *Acaa2, Acadm*/*Acadl, Hadha, Eci1/Eci2* and *Acox1* were upregulated only by 0.5 mg/g/day DT-109 (Fig. 6E and Fig. S21B). Western blot analyses showed that HADHA and ACAA2 were significantly decreased in mice fed NASH-diet and treated with H_2O or leucine, but not in mice treated glycine or DT-109. ACAA2 was significantly increased in mice treated with 0.5 mg/g/day DT-109 compared to NASH-diet H_2O control (Fig. 6F). Accordingly, the marked HS observed in livers from mice fed NASH-diet and treated with H_2O or leucine was attenuated by glycine or DT-109 (Fig. 6G, H, Fig. S21C). Particularly, diacylglycerols (DAG), which are known to promote NASH (2), were significantly reduced by 0.5 mg/g/day DT-109 (P=0.0120, Fig. 6I). To test whether the upregulation of FAO-related genes was caused directly by DT-109 treatment, we evaluated gene expression and lipid profile in livers from mice treated with DT-109 for 10 weeks on CD. Similar to the findings in mice on NASH-diet, genes regulating FAO were upregulated and liver TGs were reduced in mice treated with DT-109 on CD (Fig. 6J, K). Supporting the RNA-sequencing, qPCR, and Western blot analyses, Seahorse assays demonstrated increased oxygen consumption rate (OCR) in HepG2 cells treated with DT-109 for 24 h, which was attenuated by blocking FAO using the CPT1a inhibitor etomoxir (Fig. 6L). Thus, glycine-based treatment induces FAO and reduces NASH-diet-induced HS and lipotoxicity.

DT-109 induces hepatic *de novo* synthesis of GSH

The pathway analysis indicated increased GSH metabolism in livers from mice treated with DT-109 (Fig. 6C). RNA-sequencing revealed that genes encoding for regulators of GSH metabolism (glutathione peroxidase 6 [*Gpx6*], glutathione S-transferase, theta 2 and 3 [*Gstt2/3*], glutathione S-transferase omega 1 [*Gsto1*], glutathione S-transferase, alpha 3 [*Gsta3*], glutathione S-transferase kappa 1 [*Gstk1*], microsomal glutathione S-transferase 1 [*Mgst1*] and N-acetyltransferase 8 [*Nat8*]) and key genes mediating protection against oxidant stress and lipid peroxidation (superoxide dismutase 1 and 2 [*Sod1/2*], catalase [*Cat*], thioredoxin 2 [*Txn2*], peroxiredoxin 4 and 6 [*Prdx4/6*] and paraoxonase 1, 2 and 3 [*Pon1/2/3*]) were downregulated in mice fed NASH-diet and treated with H_2O or leucine, which was attenuated by glycine or DT-109 (Fig. 7A). qPCR analyses confirmed that *Gstt2*,

Gstt3, *Gsta3* and *Nat8* were upregulated by glycine or DT-109, whereas *Prdx4*, *Sod2* and *Txn2* were upregulated only by DT-109 (Fig. 7B). In line with these findings, assessment of lipid peroxidation using thiobarbituric acid reactive substances (TBARS) revealed increased malondialdehydes (MDA) concentrations in livers from mice fed NASH-diet and treated with H_2O or leucine that were attenuated by glycine or DT-109 (Fig. 7C). To explore the contribution of glycine-based treatment to *de novo* GSH synthesis, we performed metabolic flux analysis in AML-12 hepatocytes using $^{13}C_5$-labeled glutamine in the presence or absence of glycine or DT-109 (Fig. 7D). The cellular uptake of glycine and DT-109 was confirmed by LC-MS analysis (Fig. 7E, F). In *de novo* synthesized GSH, incorporation of $^{13}C_5$-glutamine generates a +5 mass (M+5) shift that can be detected by LC-MS. In the absence of glycine or DT-109, GSH precursors glutamate and γ-glutamylcysteine accumulated (Fig. 7G, H), indicating a block that was released upon glycine or DT-109 addition. Indeed, GSH was significantly increased ($P<0.01$) in cells treated with glycine or DT-109 (Fig. 7I), particularly M+5 GSH (Fig. 7J), indicating *de novo* synthesis of GSH. Next, to test whether DT-109 contributes to hepatic GSH formation *in vivo*, we performed a time course study in which livers were collected from mice before and after oral administration of DT-109. A significant increase in hepatic GSH was noted after 60 and 120 min ($P<0.05$, Fig. 7K). Last, similar to mice fed NASH-diet, genes regulating GSH metabolism were upregulated in livers from mice treated with DT-109 on CD (Fig. 7L). Thus, glycine-based treatment induces antioxidant defense via *de novo* GSH synthesis.

DT-109 reduces hepatic inflammation and fibrosis induced by NASH-diet

Our RNA-sequencing analysis revealed suppression of key inflammatory pathways/genes by glycine-based treatment, suggesting anti-inflammatory roles. Indeed, immunostaining for F4/80, a well-established marker for hepatic macrophages, was markedly increased in livers from mice treated with H_2O or leucine on NASH-diet, but attenuated by glycine or DT-109 (Fig. 8A, B). In plasma, monocyte chemoattractant protein-1 (MCP-1/CCL2) and resistin, known inflammatory markers in patients with NASH (39, 40), were increased in mice fed NASH-diet and treated with H_2O or leucine, but not in mice treated glycine or DT-109 (Fig. 8C, D). Plasma MCP-1 concentrations were significantly decreased in mice treated with 0.5 mg/g/day DT-109 compared to NASH-diet H_2O control (Fig. 8C). Accordingly, RNA-sequencing revealed that genes encoding for pro-inflammatory signaling regulators (*Nfkb1*/*Nfkb2*, *Relb*, *Ccr1*/*Ccr2*/*Ccr5*, *Tlr1*/*Tlr2*/ *Tlr4*, and *Tnfrsf1a* /*Tnfrsf9*/*Tnfrsf12*) and cytokines (*Tnf* and *Ccl2*/*Ccl5*) were upregulated in mice fed NASH-diet and treated with H_2O or leucine and attenuated by glycine or DT-109 (Fig. 6D). qPCR analyses confirmed that *Nfkb2*, *Relb,* and *Tnf* were significantly downregulated by glycine or DT-109 ($P<0.05$), whereas *Ccl2* and *Ccr5*, which are considered as targets for NASH treatment (2), were downregulated only by 0.5 mg/g/day DT-109 (Fig. 8E). Thus, glycine-based treatment reduces NASH-diet induced systemic and lobular inflammation and suppresses NF-κB target genes.

RNA-sequencing also demonstrated that pathways/genes related to TGFβ signaling (*Tgfb1*/*2*/*3* and *Tgfbr1/2*) and ECM remodeling (*Col1a1*/*Col1a2*/*Col3a1*/*Col4a1*/*Col4a2*, *Timp1* and *Serpine1*) were upregulated by NASH-diet and attenuated by glycine or DT-109 (Fig. 6C, D). Indeed, histological analysis based on Sirius Red revealed protective effects of

glycine or DT-109, but not leucine, against NASH-diet-induced hepatic fibrosis (Fig. 8A, F, G). These results together with the positive and significant correlations between plasma AST, ALT or ALP and individual fibrosis scores (P<0.0001), indicate that glycine or DT-109 attenuated NASH-diet-induced liver damage. To test whether glycine-based treatment attenuates TGFβ-mediated hepatic fibrosis, we analyzed SMAD signaling and found reduced SMAD2 Ser465/467 phosphorylation, mainly by DT-109 (Fig. 8H). qPCR analyses confirmed that TGFβ-related genes were markedly upregulated in livers from mice fed NASH-diet and administered H_2O or leucine which was attenuated by DT-109 (Fig. 8I). Thus, consistent with reduced lipotoxicity and oxidant stress (2), glycine-based treatment lowers NASH-diet-induced steatohepatitis and fibrosis.

Discussion

Perturbations in amino acid metabolism were suggested to be implicated in NAFLD and NASH (38, 41, 42). Particularly, lower circulating glycine has been consistently reported in patients with NAFLD (7–9), but the mechanisms behind reduced glycine and its potential as a causative factor or as a therapeutic target had not been systematically addressed so far. Herein, we identified impaired glycine biosynthesis in human and murine NAFLD. Using genetic and dietary approaches to limit glycine availability, we provide evidence for a causative role of glycine in NAFLD. In a search for potential glycine-based therapies for NAFLD, we identified DT-109 as having dual glucose/lipid-lowering effects and potently protecting mice from diet-induced NASH.

Our findings indicate that lower glycine found in NAFLD is associated with suppression of hepatic glycine biosynthetic genes. Particularly, both in murine and human NASH, we found a marked suppression of *AGXT1*, which catalyzes the conversion of glyoxylate to glycine (16, 31, 32), and showed that *AGXT1* expression inversely correlated with hepatic fat in humans. Although others reported that *AGXT1* is suppressed in patients with NASH (43) and murine models (44, 45), our work underscores a causative role for *AGXT1* in NAFLD. Proteomics of livers from $Agxt1^{-/-}$ mice indicated alterations in glucose and lipid metabolic pathways (46), but the role of AGXT1 in NASH had not been evaluated before. Using CRISPR/Cas9, we generated $Agxt^{-/-}$mice that presented exacerbated NASH after 12 weeks on NASH-diet. We identified suppression of FAO pathways that in turn promotes steatohepatitis and fibrosis (2) in $Agxt1^{-/-}$ mice, supporting the premise that impaired glycine metabolism plays a causative role in NASH.

We further applied dietary approaches to limit glycine availability and used $Apoe^{-/-}$ mice fed WD with or without glycine, allowing the simultaneous study of dyslipidemia, impaired glucose tolerance, and HS (25, 34). The enhanced adiposity, hyperlipidemia, hyperglycemia and HS observed in mice fed glycine-deficient WD are supported by previous reports in which dietary glycine accelerated fat loss (20, 22), improved glucose tolerance (20–22), reduced plasma lipids (19, 21, 22), or HS (21) in different rodent models. These findings suggest a causative role for glycine deficiency in NAFLD and, simultaneously, constitute a strong rationale to test its therapeutic potential. Here, in a thorough investigation using a long-term dietary model of advanced NAFLD featuring coexistence of steatohepatitis and fibrosis, which better mimics the human disease, we document protective effects of glycine.

In previous studies, glycine was administered to rodents via their drinking water or diet (19–22). To enhance the translational value of the current study, we applied daily and controlled oral administration of glycine to the mice. Whereas the above studies demonstrated glucose/lipid-lowering and hepatoprotective effects using higher glycine doses (≥1 mg/g/day, *19*–*22*), we report here protective effects in the NASH model at a lower dose of 0.33 mg/g/day. Considering a 12.3 dose conversion factor between mice and humans (47), our findings suggest that a minimum of 27 mg/kg/day of glycine may have beneficial effects in humans. Although the potential benefits of glycine administration to patients with NAFLD and evaluation of the optimal doses had not been reported yet, treatment of T2D patients with 5 g/day (~70 mg/kg/day) of glycine for 3 months lowered glycemia and pro-inflammatory cytokines (18), further underscoring its potential clinical benefits. We note that supplementation with 200 mg/kg/day of the glycine precursor, serine, was shown to reduce HS and plasma liver enzymes in patients with NAFLD, although with a small cohort and a short treatment period (8).

In a search for glycine-based compounds more potent than glycine for the dual glucose/lipid-lowering effects, we tested combinations of glycine with leucine, another amino acid previously reported to improve glucose tolerance and reduce HS in mice (35). Applying various T2D models, our lab uncovered potent glucose-lowering effects for the tripeptide DT-109 that exceeded those of free glycine, leucine, or their dipeptide combinations (36). Herein, we show that DT-109 also improves lipid profile, HS, and NASH using hyperlipidemia and NAFLD murine models. Unlike previously reported (35), we did not observe substantial effects in mice treated with leucine, which could be explained by the lower dose used in the current study. However, metabolic benefits were evident following glycine treatment. Also, profound benefits were noted with the lower dose of DT-109 (0.125 mg/g/day). Of note, treatment with DT-109 at 0.5 mg/g/day prevented NASH-diet-induced alternations in body composition, and reduced liver DAG and NAS, indicating that DT-109 was more potent than equivalent amounts of glycine in protecting against diet-induced NASH.

The gut microbiome has been proposed as a potential therapeutic target in NAFLD (5). Changes in fecal microbiota of patients with NAFLD affect hepatic lipid metabolism and inflammation in association with dysregulated amino acid metabolism (38). To address the mechanisms by which glycine-based treatment protects against diet-induced NASH we applied several approaches including unbiased metagenomics. We found that *Clostridiales* and *Clostridiaceae-1* were the most overrepresented order and family, respectively, in mice with NASH, mirroring previous studies in patients with NAFLD (48, 49). Furthermore, we found a marked overrepresentation of the genus *Clostridium sensu stricto* in NASH which correlated with various NAFLD-related parameters. The decrease in *Clostridium sensu stricto* during glycine-based treatment further indicates an important role for this genus in NAFLD. In support, studies in mice with diet-induced NAFLD showed that *Clostridium sensu stricto* was markedly decreased in response to antioxidant treatment (tempol) that potently reduced HS (50). In contrast, the genus *Alistipes* was overrepresented on CD or during DT-109 treatment and was inversely associated with NAS. This is consistent with previous studies reporting lower *Alistipes* abundance in patients with NAFLD (48), NASH (51), and cirrhosis (52).

By studying the effects of DT-109 on the gut microbiome independent of NASH, we found dual glucose/lipid-lowering effects also on CD. However, compared to the NASH study, minor similarities in the gut microbiome were noted in response to DT-109 treatment. DT-109 treatment caused a phylum-level change of increased *Bactriodetes* and decreased *Firmicutes*, which is commonly seen in healthy humans or animals compared to those with obesity or metabolic syndrome (53–55). However, this phylum-level change was not observed in mice treated with DT-109 on NASH-diet. Furthermore, while mildly reducing the abundance of *Clostrdium sensu stricto* on CD, DT-109 treatment did not increase the abundance of *Alistepes*. These findings indicate that the different gut microbiome observed on NASH-diet is unlikely to be the result of a direct effect of DT-109, and that alteration of the gut microbiome may not be the main mechanism by which DT-109 protects against diet-induced NASH.

Hepatic overload of free fatty acids is central to the pathogenesis of NASH. When free fatty acids are supplied to the liver in excess or their disposal via FAO is impaired, they are used as substrates for lipotoxic species that induce oxidant stress and pro-inflammatory/pro-fibrogenic pathways, promoting steatohepatitis and fibrosis (2). Our transcriptomics analysis showed that FAO was among the most suppressed pathways in livers from mice with NASH, which was reversed by DT-109 with subsequent reduction in HS and lipotoxicity. Unlike the gut microbiome, the effects of DT-109 on FAO were found to be independent of NASH, as liver TGs were reduced and FAO-related genes were upregulated also in *Apoe*$^{-/-}$ mice on WD and in wild-type mice on CD. In support, glycine intake was previously reported to increase FAO indices in livers from sucrose-fed rats (22). The *in vivo* evidence together with the metabolic assays using Seahorse indicate increased FAO as a central mechanism by which glycine-based treatment protects against NASH.

Enhancing FAO together with increasing GSH availability has been proposed as a potential strategy for NAFLD treatment (8). Glycine is the final amino acid precursor necessary for GSH synthesis (16). Both in NAFLD and T2D, GSH synthesis is diminished due to limited glycine availability and is restored following dietary supplementation (8, 56). Herein, transcriptomics showed that GSH metabolism was suppressed in NASH and was restored by glycine-based treatment that reduced hepatic lipid peroxidation. Appling metabolomics *in vivo* and *in vitro*, we found that DT-109 directly contributed to *de novo* GSH synthesis. Unlike its effects on the microbiome, the effects of DT-109 on FAO and GSH were independent of NASH. Thus, our studies indicate that glycine-based treatment induces hepatic FAO and stimulates GSH synthesis, lowering HS and lipotoxicity, which in turn attenuates NASH progression (2). Indeed, using our model, we found that glycine-based treatment attenuated NASH-diet-induced hepatic/systemic inflammation and fibrosis as evident by histological, transcriptomics, and plasma analyses.

Our study has some limitations that, in turn, may serve as future avenues of research. The human studies were limited to transcriptomics and focused on altered expression of genes regulating glycine metabolism in association with NAFLD. Future clinical studies are warranted to evaluate the potential of glycine-based treatment against NAFLD. Although we used a prolonged high-fat, cholesterol, and fructose dietary model in which mice develop both histologic and metabolic features of human NASH (2), other models could be used to

study the effects of DT-109. By studying the effects of DT-109 both in mice with NASH and in healthy mice, we found similar physiological outcomes including reduction of circulating glucose, lipids, and hepatic fat, while inducing FAO and GSH synthesis in the liver. Because we found differences in DT-109-dependent changes in the gut microbiome from mice with NASH versus healthy mice, we focused on the liver to study the mechanisms by which DT-109 protects against NASH. Nevertheless, some aspects related to the gut microbiome warrant further research. Clarifying whether DT-109 can directly and differentially affect the microbiome in relation to the host physiology could be evaluated in future studies focusing specifically on the effects of DT-109 on the gut microbiome and its metabolome. *In vitro* cultures of microbiota with DT-109 could be set up to address how the microbiota is affected by the compound without the confounding factor of the host physiology, thus, disentangling host and microbiota effects. Furthermore, evaluating putative causative roles of *Clostridium sensu stricto* or *Alistipes*, which were previously associated with liver disease (48, 50–52), could improve our understanding of the microbiome contribution to NAFLD and may lead to new diagnostics and therapeutics.

Our findings may have translational potential for the clinical management of NAFLD, currently without approved treatments. In humans, although with small sample sizes and not including patients with NASH, glycine-based treatments were shown to improve glycemic control (17, 18), lower pro-inflammatory markers (18) and reduce HS (8). Furthermore, glycine is well tolerated and safe even at high doses (57). Therefore, the therapeutic potential of DT-109 in NAFLD warrants further clinical evaluation.

Materials and Methods

Study design

The objectives of this study were to assess whether glycine metabolism is impaired in human and murine NAFLD, to evaluate glycine-based treatments in mice using models of NAFLD or hyperlipidemia, and to identify treatment mechanisms of action. DEG in livers from NASH vs. healthy cases were analyzed using human datasets (26, 27) or our previous mouse transcriptomics data (25). To test correlations between gene expression and hepatic fat content in humans, we used our previously published dataset (28). Based on those analyses which pointed at *AGXT1*, we generated *Agxt1*$^{-/-}$ mice to study diet-induced NASH. We developed glycine-modified diets to study the effects of dietary glycine in hyperlipidemic *Apoe*$^{-/-}$ mice. A search for compounds structurally similar to glycine was conducted and glucose/lipid lowering properties were tested using OGTT and in WD-fed hyperlipidemic mice. The therapeutic potential of DT-109 against NASH, was evaluated using a long-term mouse model of advanced NAFLD featuring coexistence of steatohepatitis and fibrosis (25). Sample size for mouse experiments was computed by WinPepi statistical software on the basis of pilot experiments and previous studies (25), ensuring a power of 90% and a significance of 5%. The following procedures were conducted by technicians blinded to mouse genotypes or experimental groups: histology, plasma analyses (lipid and amino acid profiles, liver enzymes and cytokines), RNA-sequencing, 16S rDNA sequencing, CLAMS, and body composition.

Animals

Animal procedures were approved (PRO00008239) by the Institutional Animal Care & Use Committee of the University of Michigan (U-M) and performed in accordance with the institutional guidelines. Seven week-old C57BL/6J (Stock: 000664) or *Apoe*$^{-/-}$ mice (B6.129P2-*Apoe*^{tm1Unc}/J, Stock: 002052) were from Jackson Laboratories. *Agxt1*$^{-/-}$ mice on the C57BL/6J background were generated using CRISPR/Cas9, with guide-RNA targeting exon 1 of *Agxt1*: 5'-GGGTCCGGGGCCCTCCAACC-3'. We performed genotyping using the following primers: forward: 5'-ACACCTCCACTGTCCTGTCC-3', reverse: 5'-GGTCAGATCTGCCTGCTACC-3'. Sanger sequencing using the following primer: 5'-GCAGAGCTAGCTGGGAAATG-3' confirmed A deletion 3 bases from the PAM (Fig. 2F). The frame-shift mutation after AA 53 of the ORF, introduced a premature stop-codon, and the absence of AGXT1 was confirmed by Western blot. AGXT1 catalyzes the biosynthesis of glycine from alanine and glyoxylate. In the absence of AGXT1, glyoxylate is accumulated and rapidly converted to oxalate (16, 31–33). The lower ratio of glycine to oxalate confirmed impaired AGXT1 activity. No CRISPR off-target effects were detected as assessed using CRISPOR (58). Eight-week old male C57BL/6J, *Apoe*$^{-/-}$, *Agxt1*$^{+/+}$ and *Agxt1*$^{-/-}$ mice were used throughout, and fed ad libitum either standard CD (LabDiet, 13% of calories from fat), high-fat, high-cholesterol WD (Envigo, 42% fat), AA-defined WD with or without glycine (developed with Envigo-Teklad Custom Diets, Table S2): WD_{AA}+Gly or WD_{AA}−Gly. For NASH studies, we used NASH-diet (Research Diets, 40% fat) that we previously confirmed to potently induce NASH in mice after 24 weeks (25) or low fat control diet (Research Diets, 10% fat). When indicated, mice were orally gavaged with glycine, N-methylglycine, N,N-dimethylglycine, N,N,N-trimethylglycine, glycolic acid, leucine (Sigma-Aldrich), DT-109, previously named Diapin (36) or DT-110 (Beijing SL Pharmaceutical) at 0.125–1 mg/g body weight/day or H_2O as control.

Human Data

Differentially expressed glycine metabolism genes in patients with NASH were analyzed using two public datasets. The first study (26) consists of liver microarray data obtained from 104 patients with NASH and 44 normal controls (GSE83452). The second dataset (27) includes liver microarray data collected from 24 patients with NASH and 24 heathy obese controls (GSE61260). We used a linear regression model with age, sex, and BMI as covariates to identify significant glycine metabolism genes that are associated with NASH: Gene expression=β_NASH*NASH status+ β_Age*Age+β_Sex*Sex+β_BMI*BMI+ ε, where NASH status was coded as 1 for NASH and 0 for healthy controls. To increase the statistical power and compare the results, we further performed a meta-analysis of the two studies with a fixed effect model using the metafor R package. Genes with Benjamini-Hochberg adjusted *P* value <0.05 and Cochran's Q heterogeneity test *P* value >0.05 were considered as significant. Spearman's correlations between gene expression and hepatic fat content were tested using our previously published microarray data (28) collected from liver transplantation donors (n=206, GSE26106). The tissue dissection, sample exclusion, and microarray data generation were performed as previously described (28, 59). The hepatic fat content of livers was quantified using hexane/isopropanol (3:2), as described previously (28, 60). The extracted total fat content was normalized to total protein concentration and transformed to log10 scale for the subsequent analysis. Spearman's correlation was used to

determine the significance of the hepatic fat correlated with expression of glycine biosynthetic genes.

Statistical analysis

Statistical analyses were performed using GraphPad Prism 8.0. All data were tested for normality and equal variance. If passed, Student's t test was used to compare two groups or one-way ANOVA followed by Bonferroni post-hoc test for comparisons among >2 groups. Otherwise, nonparametric tests (Mann-Whitney U test or Kruskal-Wallis test followed by Dunn's post-hoc test) were used. P value <0.05 was considered statistically significant.

Supplementary Material

Refer to Web version on PubMed Central for supplementary material.

Acknowledgments:

We thank M. Pietzke and A. Vazquez for their help in visualization of metabolomics data using Metabolite Autoplotter. We utilized services from the U-M In-Vivo Animal Core supported by grant U2CDK110768, the Metabolomics Core supported by grant U24DK097153, and the Animal Phenotyping Core supported by grants DK020572, DK089503 and 1U2CDK110678-01.

Funding: This study was supported by the National Institute of Health (NIH) grants HL150233 (O.R.), HL123333 (L.V.), HL138139 (J.Z.), DK106540 (W.L.), HL137214, HL068878 and HL134569 (Y.E.C.), the American Heart Association Postdoctoral Fellowship 19POST34380224 (O.R.), the Michigan-Israel Partnership for Research and Education (O.R., T.H., M.A., E.G., I.M., Y.E.C.), Michigan Center for Therapeutic Innovation (J.C.R.), the Israeli Centers of Research Excellence (I-CORE) program (Center No. 1775/12, I.M.) and the Israel Science Foundation (ISF, grant No. 824/19, I.M.).

References and Notes:

1. Younossi ZM, Koenig AB, Abdelatif D, Fazel Y, Henry L, Wymer M. Global epidemiology of nonalcoholic fatty liver disease-Meta-analytic assessment of prevalence, incidence, and outcomes. Hepatology. 64, 73–84 (2016). [PubMed: 26707365]
2. Friedman SL, Neuschwander-Tetri BA, Rinella M, Sanyal AJ. Mechanisms of NAFLD development and therapeutic strategies. Nat. Med 24, 908–922 (2018). [PubMed: 29967350]
3. Bedossa P, Poitou C, Veyrie N, Bouillot JL, Basdevant A, Paradis V, Tordjman J, Clement K. Histopathological algorithm and scoring system for evaluation of liver lesions in morbidly obese patients. Hepatology. 56, 1751–17599 (2012). [PubMed: 22707395]
4. Sinn DH, Cho SJ, Gu S, Seong D, Kang D, Kim H, Yi BK, Paik SW, Guallar E, Cho J, Gwak GY. Persistent Nonalcoholic Fatty Liver Disease Increases Risk for Carotid Atherosclerosis. Gastroenterology. 151, 481–488.e1 (2016). [PubMed: 27283259]
5. Younes R, Bugianesi E. A spotlight on pathogenesis, interactions and novel therapeutic options in NAFLD. Nat. Rev. Gastroenterol. Hepatol 16,80–82 (2019). [PubMed: 30559444]
6. Parekh S, Anania FA. Abnormal lipid and glucose metabolism in obesity: implications for nonalcoholic fatty liver disease. Gastroenterology. 132, 2191–207 (2007). [PubMed: 17498512]
7. Yamakado M, Tanaka T, Nagao K, Imaizumi A, Komatsu M, Daimon T, Miyano H, Tani M, Toda A, Yamamoto H, Horimoto K, Ishizaka Y. Plasma amino acid profile associated with fatty liver disease and co-occurrence of metabolic risk factors. Sci. Rep 7,14485 (2017). [PubMed: 29101348]
8. Mardinoglu A, Bjornson E, Zhang C, Klevstig M, Söderlund S, Ståhlman M, Adiels M, Hakkarainen A, Lundbom N, Kilicarslan M, Hallström BM, Lundbom J, Vergès B, Barrett PH, Watts GF, Serlie MJ, Nielsen J, Uhlén M, Smith U, Marschall HU, Taskinen MR, Boren J. Personal model-assisted identification of NAD+ and glutathione metabolism as intervention target in NAFLD. Mol. Syst. Biol 13, 916 (2017). [PubMed: 28254760]

9. Gaggini M, Carli F, Rosso C, Buzzigoli E, Marietti M, Della Latta V, Ciociaro D, Abate ML, Gambino R, Cassader M, Bugianesi E, Gastaldelli A. Altered amino acid concentrations in NAFLD: Impact of obesity and insulin resistance. Hepatology. 67, 145–158 (2018). [PubMed: 28802074]
10. Zhou Y, Orešič M, Leivonen M, Gopalacharyulu P, Hyysalo J, Arola J, Verrijken A, Francque S, Van Gaal L, Hyötyläinen T, Yki-Järvinen H. Noninvasive Detection of Nonalcoholic Steatohepatitis Using Clinical Markers and Circulating Levels of Lipids and Metabolites. Clin. Gastroenterol. Hepatol 14, 1463–1472.e6 (2016). [PubMed: 27317851]
11. Newgard CB, An J, Bain JR, Muehlbauer MJ, Stevens RD, Lien LF, Haqq AM, Shah SH, Arlotto M, Slentz CA, Rochon J, Gallup D, Ilkayeva O, Wenner BR Jr., Yancy WS, Eisenson H, Musante G, Surwit RS, Millington DS, Butler MD, Svetkey LP. A branched-chain amino acid-related metabolic signature that differentiates obese and lean humans and contributes to insulin resistance. Cell Metab. 9, 311–326 (2009). [PubMed: 19356713]
12. Guasch-Ferré M, Hruby A, Toledo E, Clish CB, Martínez-González MA, Salas-Salvadó J, Hu FB. Metabolomics in Prediabetes and Diabetes: A Systematic Review and Meta-analysis. Diabetes Care. 39, 833–846 (2016). [PubMed: 27208380]
13. Li X, Sun L, Zhang W, Li H, Wang S, Mu H, Zhou Q, Zhang Y, Tang Y, Wang Y, Chen W, Yang R, Dong J. Association of serum glycine levels with metabolic syndrome in an elderly Chinese population. Nutr. Metab. (Lond) 15, 89 (2018). [PubMed: 30568717]
14. Ding Y, Svingen GF, Pedersen ER, Gregory JF, Ueland PM, Tell GS, Nygård OK. Plasma Glycine and Risk of Acute Myocardial Infarction in Patients With Suspected Stable Angina Pectoris. J. Am. Heart Assoc 5, pii: e002621 (2015). [PubMed: 26722126]
15. Wittemans LBL, Lotta LA, Oliver-Williams C, Stewart ID, Surendran P, Karthikeyan S, Day FR, Koulman A, Imamura F, Zeng L, Erdmann J, Schunkert H, Khaw KT, Griffin JL,Forouhi NG, Scott RA, Wood AM, Burgess S, Howson JMM, Danesh J, Wareham NJ, Butterworth AS, Langenberg C. Assessing the causal association of glycine with risk of cardio-metabolic diseases. Nat. Commun 10, 1060 (2019). [PubMed: 30837465]
16. Wang W, Wu Z, Dai Z, Yang Y, Wang J, Wu G. Glycine metabolism in animals and humans: implications for nutrition and health. Amino Acids. 45,463–477 (2013). [PubMed: 23615880]
17. Gannon MC, Nuttall JA, Nuttall FQ. The metabolic response to ingested glycine. Am. J. Clin. Nutr 76, 1302–1307 (2002). [PubMed: 12450897]
18. Cruz M, Maldonado-Bernal C, Mondragón-Gonzalez R, Sanchez-Barrera R, Wacher NH, Carvajal-Sandoval G, Kumate J. Glycine treatment decreases proinflammatory cytokines and increases interferon-gamma in patients with type 2 diabetes. J. Endocrinol. Invest 31, 694–699 (2008). [PubMed: 18852529]
19. Rom O, Grajeda-Iglesias C, Najjar M, Abu-Saleh N, Volkova N, Dar DE, Hayek T, Aviram M. Atherogenicity of amino acids in the lipid-laden macrophage model system in vitro and in atherosclerotic mice: a key role for triglyceride metabolism. J. Nutr. Biochem 45, 24–38 (2017). [PubMed: 28431321]
20. Caldow MK, Ham DJ, Godeassi DP, Chee A, Lynch GS, Koopman R. Glycine supplementation during calorie restriction accelerates fat loss and protects against further muscle loss in obese mice. Clin. Nutr 35, 1118–1126 (2016). [PubMed: 26431812]
21. Takashima S, Ikejima K, Arai K, Yokokawa J, Kon K, Yamashina S, Watanabe S. Glycine prevents metabolic steatohepatitis in diabetic KK-Ay mice through modulation of hepatic innate immunity. Am. J. Physiol. Gastrointest. Liver Physiol 311, G1105–G1113 (2016). [PubMed: 27659424]
22. El Hafidi M, Pérez I, Zamora J, Soto V, Carvajal-Sandoval G, Baños G. Glycine intake decreases plasma free fatty acids, adipose cell size, and blood pressure in sucrose-fed rats. Am. J. Physiol. Regul. Integr. Comp. Physiol 287, R1387–1393 (2004). [PubMed: 15331379]
23. Rom O, Villacorta L, Zhang J, Chen YE, Aviram M. Emerging therapeutic potential of glycine in cardiometabolic diseases: dual benefits in lipid and glucose metabolism. Curr. Opin. Lipidol 29, 428–432 (2018). [PubMed: 30153136]
24. Bruck R, Wardi J, Aeed H, Avni Y, Shirin H, Avinoach L, Shahmurov M, Hershkoviz R. Glycine modulates cytokine secretion, inhibits hepatic damage and improves survival in a model of endotoxemia in mice. Liver Int. 23, 276–282 (2003). [PubMed: 12895268]

25. Rom O, Xu G, Guo Y, Zhu Y, Wang H, Zhang J, Fan Y, Liang W, Lu H, Liu Y, Aviram M, Liu Z, Kim S, Liu W, Wang X, Chen YE, Villacorta L. Nitro-fatty acids protect against steatosis and fibrosis during development of nonalcoholic fatty liver disease in mice. EBioMedicine. 41, 62–72 (2019). [PubMed: 30772307]

26. Lefebvre P, Lalloyer F, Baugé E, Pawlak M, Gheeraert C, Dehondt H, Vanhoutte J, Woitrain E, Hennuyer N, Mazuy C, Bobowski-Gérard M, Zummo FP, Derudas B, Driessen A, Hubens G, Vonghia L, Kwanten WJ, Michielsen P, Vanwolleghem T, Eeckhoute J, Verrijken A, Van Gaal L, Francque S, Staels B. Interspecies NASH disease activity whole-genome profiling identifies a fibrogenic role of PPARα-regulated dermatopontin. JCI Insight. 2, pii: 92264 (2017). [PubMed: 28679947]

27. Horvath S, Erhart W, Brosch M, Ammerpohl O, von Schönfels W, Ahrens M, Heits N, Bell JT, Tsai PC, Spector TD, Deloukas P, Siebert R, Sipos B, Becker T, Röcken C, Schafmayer C, Hampe J. Obesity accelerates epigenetic aging of human liver. Proc. Natl. Acad. Sci. U. S. A 111, 15538–15543 (2014). [PubMed: 25313081]

28. Wang L, Athinarayanan S, Jiang G, Chalasani N, Zhang M, Liu W. Fatty acid desaturase 1 gene polymorphisms control human hepatic lipid composition. Hepatology. 61, 119–128 (2015). [PubMed: 25123259]

29. Montagner A, Polizzi A, Fouché E, Ducheix S, Lippi Y, Lasserre F, Barquissau V, Régnier M, Lukowicz C, Benhamed F, Iroz A, Bertrand-Michel J, Al Saati T, Cano P, Mselli-Lakhal L, Mithieux G, Rajas F, Lagarrigue S, Pineau T, Loiseau N, Postic C, Langin D, Wahli W, Guillou H. Liver PPARα is crucial for whole-body fatty acid homeostasis and is protective against NAFLD. Gut. 65, 1202–1214 (2016). [PubMed: 26838599]

30. Seki E, De Minicis S, Osterreicher CH, Kluwe J, Osawa Y, Brenner DA, Schwabe RF. TLR4 enhances TGF-beta signaling and hepatic fibrosis. Nat. Med 13, 1324–1332 (2007). [PubMed: 17952090]

31. Lumb MJ, Danpure CJ. Functional synergism between the most common polymorphism in human alanine:glyoxylate aminotransferase and four of the most common disease-causing mutations. J. Biol. Chem 275, 36415–36422 (2000). [PubMed: 10960483]

32. Li XM, Salido EC, Shapiro LJ. The mouse alanine:glyoxylate aminotransferase gene (Agxt1): cloning, expression, and mapping to chromosome 1. Somat. Cell. Mol. Genet 25, 67–77 (1999). [PubMed: 11225057]

33. Salido EC, Li XM, Lu Y, Wang X, Santana A, Roy-Chowdhury N, Torres A, Shapiro LJ, Roy-Chowdhury J. Alanine-glyoxylate aminotransferase-deficient mice, a model for primary hyperoxaluria that responds to adenoviral gene transfer. Proc. Natl. Acad. Sci. U. S. A 103, 18249–18254 (2006). [PubMed: 17110443]

34. Schierwagen R, Maybüchen L, Zimmer S, Hittatiya K, Bäck C, Klein S, Uschner FE, Reul W, Boor P, Nickenig G, Strassburg CP, Trautwein C, Plat J, Lütjohann D, Sauerbruch T, Tacke F, Trebicka J. Seven weeks of Western diet in apolipoprotein-E-deficient mice induce metabolic syndrome and non-alcoholic steatohepatitis with liver fibrosis. Sci. Rep 11, 12931 (2015).

35. Macotela Y, Emanuelli B, Bång AM, Espinoza DO, Boucher J, Beebe K, Gall W, Kahn CR. Dietary leucine--an environmental modifier of insulin resistance acting on multiple levels of metabolism. PLoS One. 6, e21187 (2011). [PubMed: 21731668]

36. Zhang J, Xue C, Zhu T, Vivekanandan A, Pennathur S, Ma ZA, Chen YE. A tripeptide Diapin effectively lowers blood glucose levels in male type 2 diabetes mice by increasing blood levels of insulin and GLP-1. PLoS One. 8, e83509 (2013). [PubMed: 24386218]

37. Trajcevski KE, O'Neill HM, Wang DC, Thomas MM, Al-Sajee D, Steinberg GR, Ceddia RB, Hawke TJ. Enhanced lipid oxidation and maintenance of muscle insulin sensitivity despite glucose intolerance in a diet-induced obesity mouse model. PLoS One. 8, e71747 (2013). [PubMed: 23951235]

38. Hoyles L, Fernández-Real JM, Federici M, Serino M, Abbott J, Charpentier J, Heymes C, Luque JL, Anthony E, Barton RH, Chilloux J, Myridakis A, Martinez-Gili L, Moreno-Navarrete JM, Benhamed F, Azalbert V, Blasco-Baque V, Puig J, Xifra G, Ricart W, Tomlinson C, Woodbridge M, Cardellini M, Davato F, Cardolini I, Porzio O, Gentileschi P, Lopez F, Foufelle F, Butcher SA, Holmes E, Nicholson JK, Postic C, Burcelin R, Dumas ME. Molecular phenomics and

metagenomics of hepatic steatosis in non-diabetic obese women. Nat. Med 24, 1070–1080 (2018). [PubMed: 29942096]

39. Haukeland JW, Damås JK, Konopski Z, Løberg EM, Haaland T, Goverud I, Torjesen PA, Birkeland K, Bjøro K, Aukrust P. Systemic inflammation in nonalcoholic fatty liver disease is characterized by elevated levels of CCL2. J. Hepatol 44, 1167–1174 (2006). [PubMed: 16618517]
40. Pagano C, Soardo G, Pilon C, Milocco C, Basan L, Milan G, Donnini D, Faggian D , Mussap M, M Plebani C Avellini, G. Federspil, L. A. Sechi, R. Vettor. Increased serum resistin in nonalcoholic fatty liver disease is related to liver disease severity and not to insulin resistance. J. Clin. Endocrinol. Metab 91, 1081–1086 (2006). [PubMed: 16394091]
41. Mardinoglu A, Agren R, Kampf C, Asplund A, Uhlen M, Nielsen J. Genome-scale metabolic modelling of hepatocytes reveals serine deficiency in patients with non-alcoholic fatty liver disease. Nat. Commun 5, 3083 (2014). [PubMed: 24419221]
42. Sookoian S, Pirola CJ. NAFLD. Metabolic make-up of NASH: from fat and sugar to amino acids. Nat. Rev. Gastroenterol. Hepatol 11, 205–207 (2014). [PubMed: 24566880]
43. Stepanova M, Hossain N, Afendy A, Perry K, Goodman ZD, Baranova A, Younossi Z. Hepatic gene expression of Caucasian and African-American patients with obesity-related nonalcoholic fatty liver disease. Obes. Surg 20, 640–650 (2010). [PubMed: 20119733]
44. Teufel A, Itzel T, Erhart W, Brosch M, Wang XY, Kim YO, von Schönfels W, Herrmann A, Brückner S, Stickel F, Dufour JF, Chavakis T, Hellerbrand C, Spang R, Maass T, Becker T, Schreiber S, Schafmayer C, Schuppan D, Hampe J. Comparison of Gene Expression Patterns Between Mouse Models of Nonalcoholic Fatty Liver Disease and Liver Tissues From Patients. Gastroenterology. 151, 513–525 (2016). [PubMed: 27318147]
45. Asgharpour A, Cazanave SC, Pacana T, Seneshaw M, Vincent R, Banini BA, Kumar DP, Daita K, Min HK, Mirshahi F, Bedossa P, Sun X, Hoshida Y, Koduru SV Jr., Contaifer D, Warncke UO, Wijesinghe DS, Sanyal AJ. A diet-induced animal model of nonalcoholic fatty liver disease and hepatocellular cancer. J. Hepatol 65, 579–688 (2016). [PubMed: 27261415]
46. Hernández-Fernaud JR, Salido E. Differential expression of liver and kidney proteins in a mouse model for primary hyperoxaluria type I. FEBS J. 277, 4766–4774 (2010). [PubMed: 20977670]
47. Nair AB, Jacob S. A simple practice guide for dose conversion between animals and human. J. Basic Clin. Pharm 7, 27–31 (2016). [PubMed: 27057123]
48. Jiang W, Wu N, Wang X, Chi Y, Zhang Y, Qiu X, Hu Y, Li J, Liu Y. Dysbiosis gut microbiota associated with inflammation and impaired mucosal immune function in intestine of humans with non-alcoholic fatty liver disease. Sci. Rep 5, 8096 (2015). [PubMed: 25644696]
49. Raman M, Ahmed I, Gillevet PM, Probert CS, Ratcliffe NM, Smith S, Greenwood R, Sikaroodi M, Lam V, Crotty P, Bailey J, Myers RP, Rioux KP. Fecal microbiome and volatile organic compound metabolome in obese humans with nonalcoholic fatty liver disease. Clin. Gastroenterol. Hepatol 11, 868–875 (2013). [PubMed: 23454028]
50. Jiang C, Xie C, Li F, Zhang L, Nichols RG, Krausz KW, Cai J, Qi Y, Fang ZZ, Takahashi S, Tanaka N, Desai D, Amin SG, Albert I, Patterson AD, Gonzalez FJ. Intestinal farnesoid X receptor signaling promotes nonalcoholic fatty liver disease. J. Clin. Invest 125, 386–402 (2015). [PubMed: 25500885]
51. Zhu L, Baker SS, Gill C, Liu W, Alkhouri R, Baker RD, Gill SR. Characterization of gut microbiomes in nonalcoholic steatohepatitis (NASH) patients: a connection between endogenous alcohol and NASH. Hepatology. 57, 601–609 (2013). [PubMed: 23055155]
52. Qin N, Yang F, Li A, Prifti E, Chen Y, Shao L, Guo J, Le Chatelier E, Yao J, Wu L, Zhou J, Ni S, Liu L, Pons N, Batto JM, Kennedy SP, Leonard P, Yuan C, Ding W, Chen Y, Hu X, Zheng B, Qian G, Xu W, Ehrlich SD, Zheng S, Li L. Alterations of the human gut microbiome in liver cirrhosis. Nature. 513, 59–64 (2014). [PubMed: 25079328]
53. Ley RE, Bäckhed F, Turnbaugh P, Lozupone CA, Knight RD, Gordon JI. Obesity alters gut microbial ecology. Proc Natl Acad Sci U S A. 102, 11070–11075 (2005). [PubMed: 16033867]
54. Ley RE, Turnbaugh PJ, Klein S, Gordon JI. Microbial ecology: human gut microbes associated with obesity. Nature. 444, 1022–1023 (2006). [PubMed: 17183309]
55. Woting A, Blaut M. The Intestinal Microbiota in Metabolic Disease. Nutrients. 8, 202 (2016). [PubMed: 27058556]

56. Sekhar RV, McKay SV, Patel SG, Guthikonda AP, Reddy VT, Balasubramanyam A, Jahoor F. Glutathione synthesis is diminished in patients with uncontrolled diabetes and restored by dietary supplementation with cysteine and glycine. Diabetes Care. 34, 162–167 (2011). [PubMed: 20929994]
57. Heresco-Levy U, Javitt DC, Ermilov M, Mordel C, Silipo G, Lichtenstein M. Efficacy of high-dose glycine in the treatment of enduring negative symptoms of schizophrenia. Arch. Gen. Psychiatry 56, 29–36 (1999). [PubMed: 9892253]
58. Haeussler M, Schönig K, Eckert H, Eschstruth A, Mianné J, Renaud JB, Schneider-Maunoury S, Shkumatava A, Teboul L, Kent J, Joly JS, Concordet JP. Evaluation of off-target and on-target scoring algorithms and integration into the guide RNA selection tool CRISPOR. Genome Biol. 17, 148 (2016). [PubMed: 27380939]
59. Innocenti F, Cooper GM, Stanaway IB, Gamazon ER, Smith JD, Mirkov S, Ramirez J, Liu W, Lin YS, Moloney C, Aldred SF, Trinklein ND, Schuetz E, Nickerson DA, Thummel KE, Rieder MJ, Rettie AE, Ratain MJ, Cox NJ, Brown CD. Identification, replication, and functional fine-mapping of expression quantitative trait loci in primary human liver tissue. PLoS Genet. 7, e1002078 (2011). [PubMed: 21637794]
60. Li M, Song J, Mirkov S, Xiao SY, Hart J, Liu W. Comparing morphometric, biochemical, and visual measurements of macrovesicular steatosis of liver. Hum. Pathol 42, 356–360 (2011). [PubMed: 21111448]
61. Bolger AM, Lohse M, Usadel B. Trimmomatic: a flexible trimmer for Illumina sequence data. Bioinformatics. 30, 2114–2120 (2014). [PubMed: 24695404]
62. Anders S, Pyl PT, Huber W. HTSeq--a Python framework to work with high-throughput sequencing data. Bioinformatics. 31, 166–169 (2015). [PubMed: 25260700]
63. Love MI, Huber W, Anders S. Moderated estimation of fold change and dispersion for RNAseq data with DESeq2. Genome Biol.15, 550 (2014). [PubMed: 25516281]
64. Yu G, Wang LG, Han Y, He QY. clusterProfiler: an R package for comparing biological themes among gene clusters. OMICS. 16, 284–287 (2012). [PubMed: 22455463]
65. Rom O, Korach-Rechtman H, Hayek T, Danin-Poleg Y, Bar H, Kashi Y, Aviram M. Acrolein increases macrophage atherogenicity in association with gut microbiota remodeling in atherosclerotic mice: protective role for the polyphenol-rich pomegranate juice. Arch. Toxicol 91, 1709–1725 (2017). [PubMed: 27696135]
66. Wu J, Wen XW, Faulk C, Boehnke K, Zhang H, Dolinoy DC, Xi C. Perinatal Lead Exposure Alters Gut Microbiota Composition and Results in Sex-specific Bodyweight Increases in Adult Mice. Toxicol. Sci 151, 324–33 (2016). [PubMed: 26962054]
67. Schloss PD, Westcott SL, Ryabin T, Hall JR, Hartmann M, Hollister EB, Lesniewski RA, Oakley BB, Parks DH, Robinson CJ, Sahl JW, Stres B, Thallinger GG, Van Horn DJ, Weber CF CF. Introducing mothur: open-source, platform-independent, community-supported software for describing and comparing microbial communities. Appl. Environ. Microbiol 75, 7537–7541 (2009). [PubMed: 19801464]
68. Quince C, Lanzén A, Curtis TP, Davenport RJ, Hall N, Head IM, Read LF, Sloan WT. Accurate determination of microbial diversity from 454 pyrosequencing data. Nat. Methods 6, 639–641 (2009). [PubMed: 19668203]
69. Sheneman L, Evans J, Foster JA. Clearcut: a fast implementation of relaxed neighbor joining. Bioinformatics. 22, 2823–2824 (2006). [PubMed: 16982706]
70. Schloss PD, Handelsman J. Introducing TreeClimber, a test to compare microbial community structures. Appl. Environ. Microbiol 72, 2379–2384 (2006). [PubMed: 16597933]
71. Hamady M, Lozupone C, Knight R. Fast UniFrac: facilitating high-throughput phylogenetic analyses of microbial communities including analysis of pyrosequencing and PhyloChip data. ISME J. 4, 17–27 (2010). [PubMed: 19710709]
72. Blanchet FG, Legendre P, Borcard D. Forward selection of explanatory variables. Ecology. 89, 2623–2632 (2008). [PubMed: 18831183]
73. Segata N, Izard J, Waldron L, Gevers D, Miropolsky L, Garrett WS, Huttenhower C. Metagenomic biomarker discovery and explanation. Genome Biol. 12, R60 (2011). [PubMed: 21702898]

74. McMurdie PJ, Holmes S. Shiny-phyloseq: Web application for interactive microbiome analysis with provenance tracking. Bioinformatics. 31, 282–283 (2015). [PubMed: 25262154]

75. Mackay GM, Zheng LL, van den Broek NJ, Gottlieb E. Analysis of Cell Metabolism Using LC-MS and Isotope Tracers. Methods Enzymol. 561, 171–96 (2015). [PubMed: 26358905]

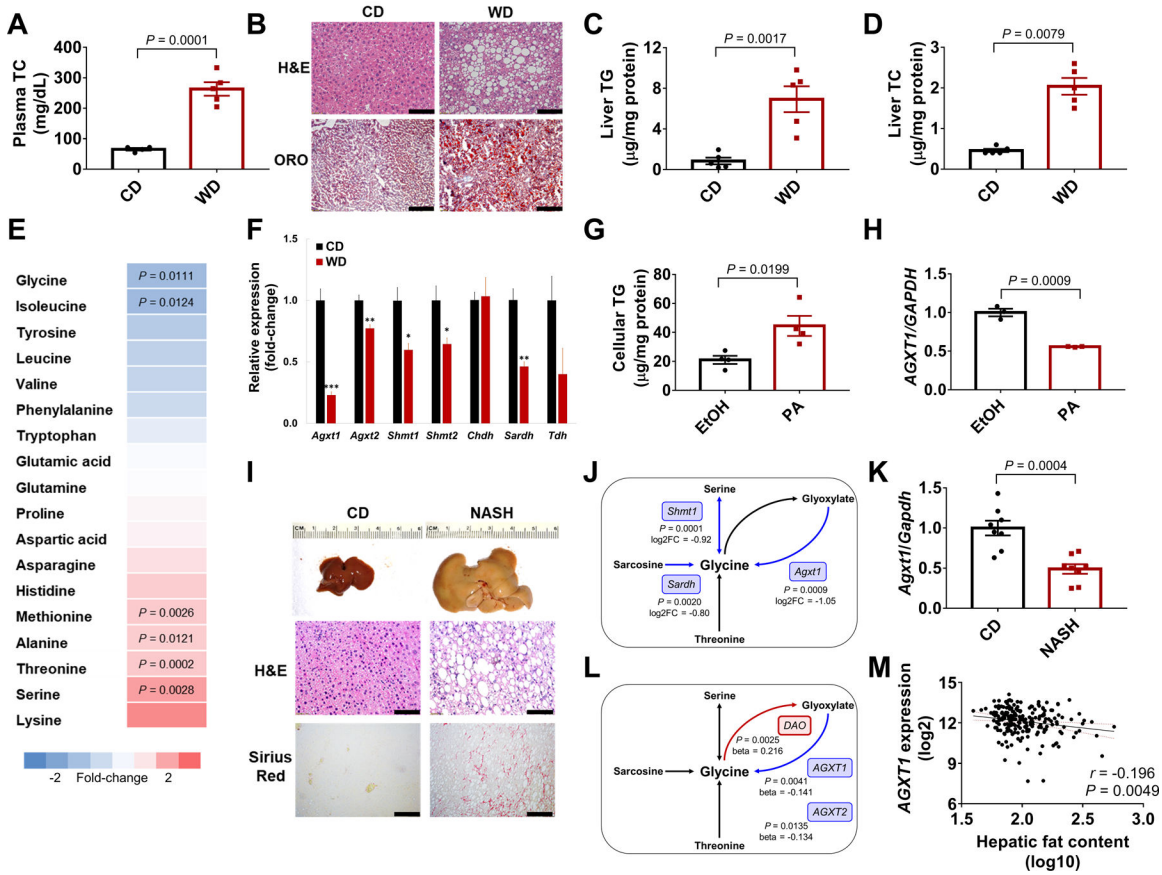

Fig. 1. Impaired glycine biosynthesis in NAFLD.

C57BL/6J mice were fed standard chow-diet (CD) or Western-diet (WD) for 12 weeks: **(A)** Plasma TC. **(B)** Liver histology (Scale bar: H&E 50µm, ORO 100µm), **(C)** TGs, **(D)** and TC. **(E)** Plasma amino acids relative to CD. **(F)** Hepatic expression of glycine biosynthetic genes relative to glyceraldehyde 3-phosphate dehydrogenase (*Gapdh),* **P*<0.05, ***P*<0.01, ****P*<0.001 vs. CD (n=4–5). **(G)** Cellular TGs and **(H)** *AGXT1* expression in HepG2 cells loaded with 200 µM PA or ethanol for 24h (n=3–4). C57BL/6J mice were fed NASH-diet or CD for 24 weeks (n=10): **(I)** Liver morphology, H&E and Sirius Red histology (Scale bar: 50 µm), **(J)** significant downregulation (blue) of glycine biosynthetic genes/pathways by RNA-sequencing of livers from CD or NASH-diet fed mice (n=3, log2FC, log2fold-change), **(K)** *Agxt1* expression relative to *Gapdh* in mice with diet-induced NASH (n=8). **(L)** Significant downregulation (blue) or upregulation (red) in glycine metabolism genes by meta-analysis of liver microarray data from healthy vs. NASH patients. **(M)** Spearman's correlation between *AGXT1* expression and hepatic fat in livers from transplantation donors (n=206). Data are means ± SEM. Statistical differences were compared using Student's t test or Mann-Whitney U test. Benjamini-Hochberg and Cochran's Q heterogeneity tests were used to determine the significance of glycine metabolism genes associated with NASH.

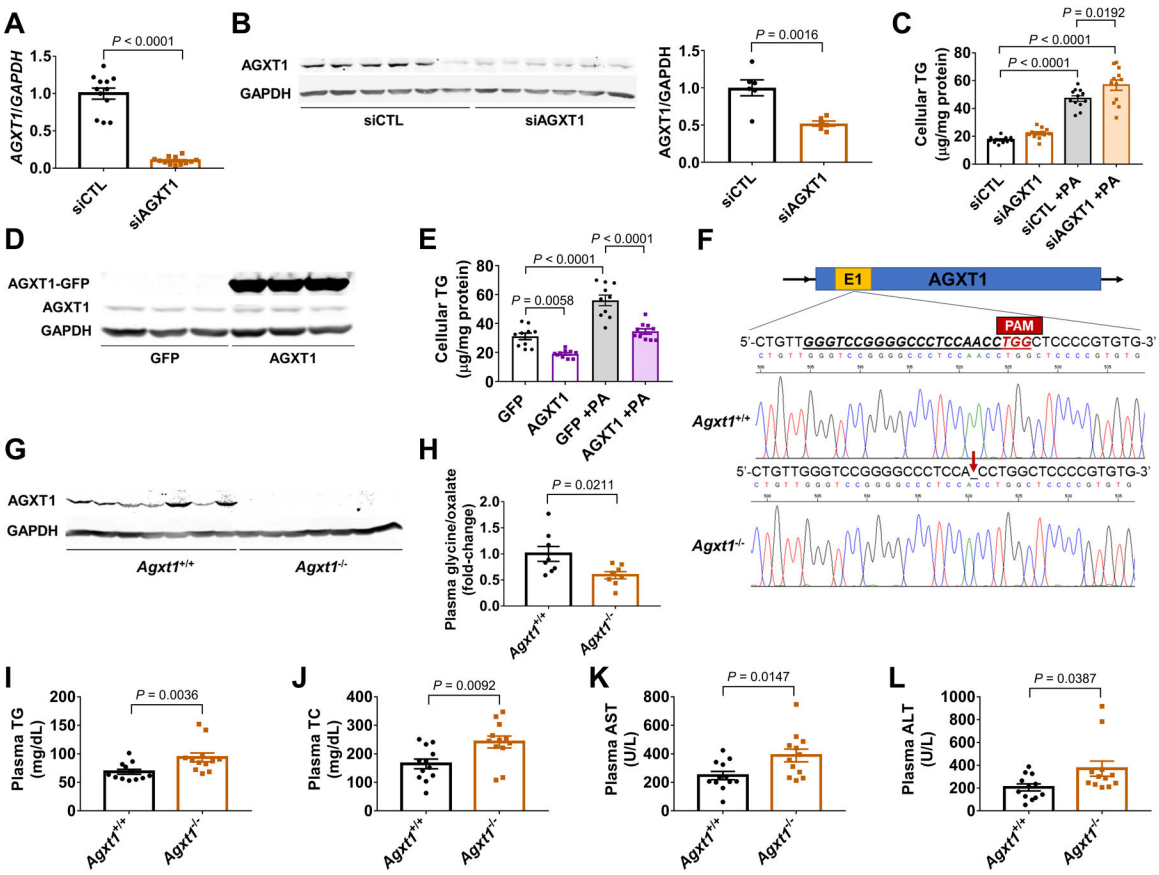

Fig. 2. Plasma alterations in *Agxt1*$^{-/-}$ mice fed NASH-diet.

HepG2 cells were transfected with siRNA targeting *AGXT1* (siAGXT1) or non-targeting siRNA control (siCTL): **(A)** *AGXT1* mRNA relative to *GAPDH* (n=12), **(B)** Western blot and quantitative densitometry of AGXT1 relative to GAPDH (n=6), and **(C)** cellular TG, with or without PA loading (200 µM, n=12). HepG2 cells were transfected with a GFP-tagged AGXT1 plasmid or a GFP plasmid as control: **(D)** Western blot of AGXT1 relative to GAPDH (n=3), and **(E)** cellular TG, with or without PA loading (200 µM, n=10). **(F)** CRISPR/Cas9 strategy to generate *Agxt1*$^{-/-}$ mice. The guide-RNA target site on exon 1 of *Agxt1* is underlined. A deletion three bases from the protospacer adjacent motif (PAM) was confirmed by Sanger sequencing. **(G)** Absence of AGXT1 confirmed by Western blot (n=7). *Agxt1*$^{+/+}$ and *Agxt1*$^{-/-}$ mice were fed NASH-diet for 12 weeks: Plasma **(H)** glycine/oxalate ratio (n=8), **(I)** TG, **(J)** TC, **(K)** AST and **(L)** ALT (n=12). Data are means ± SEM. Statistical differences were compared using Student's t test or Mann-Whitney U test.

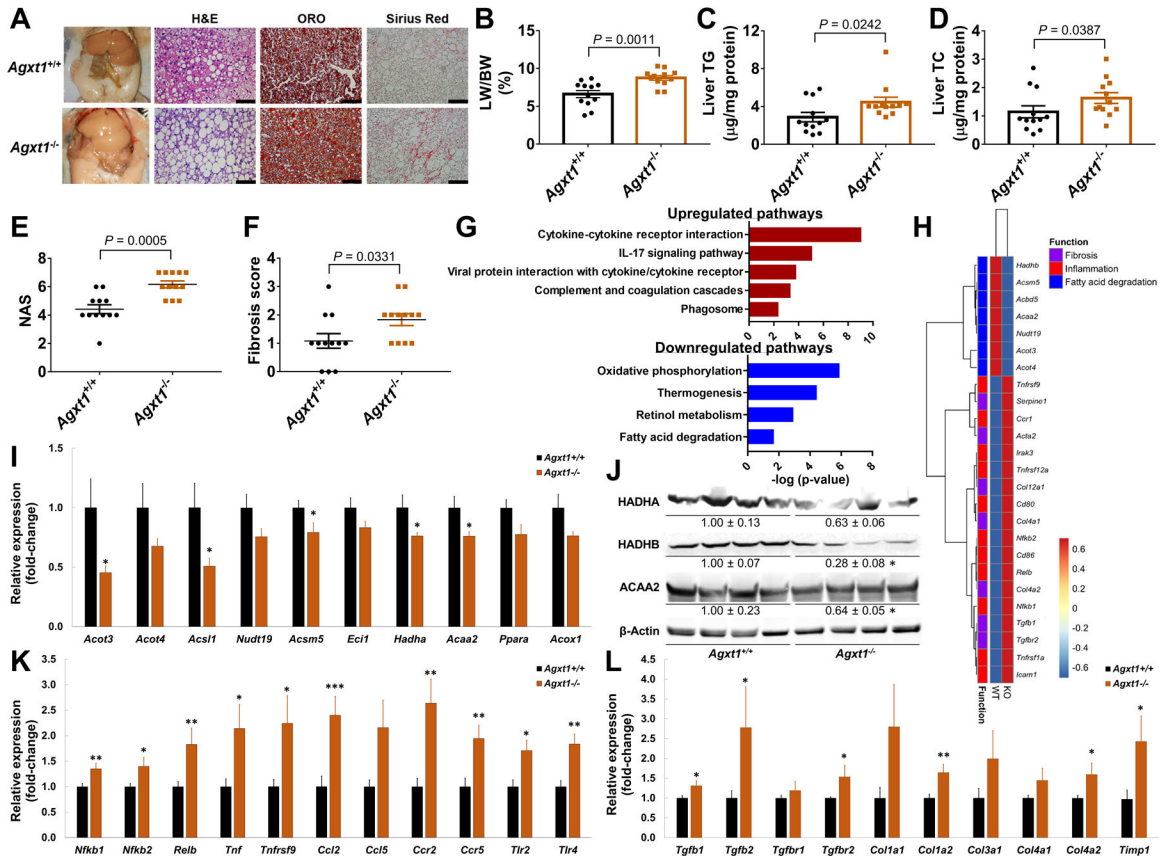

Fig. 3. Accelerated diet-induced NASH in *Agxt1*$^{-/-}$ mice.

Agxt1$^{+/+}$ and *Agxt1*$^{-/-}$ mice were fed NASH-diet for 12 weeks (n=12): **(A)** Gross appearance of the peritoneal cavities and liver histology (Scale bar: H&E and Sirius Red 50µm, ORO 100µm), **(B)** liver weight/body weight ratio (LW/BW %), **(C)** liver TG, **(D)** liver TC, **(E)** NAS and **(F)** fibrosis score. **(G)** Pathway analysis following RNA-sequencing of livers from *Agxt1*$^{+/+}$ and *Agxt1*$^{-/-}$ mice (n=4). Pathways enriched in the up- or down-regulated DEG are plotted in red or blue, respectively. **(H)** Heatmap of NASH-related DEG. **(I)** FAO-related DEG confirmed by qPCR (n=10) and **(J)** Western blot (n=4). **(K)** Inflammation- and **(L)** fibrosis-related DEG confirmed by qPCR (n=10). *P<0.05, **P<0.01, ***P<0.001 vs. *Agxt1*$^{+/+}$. Data are means ± SEM. Statistical differences were compared using Student's t test or Mann-Whitney U test. The significance of the enriched pathways was determined by right-tailed Fisher's exact test followed by Benjamini-Hochberg multiple testing adjustment.

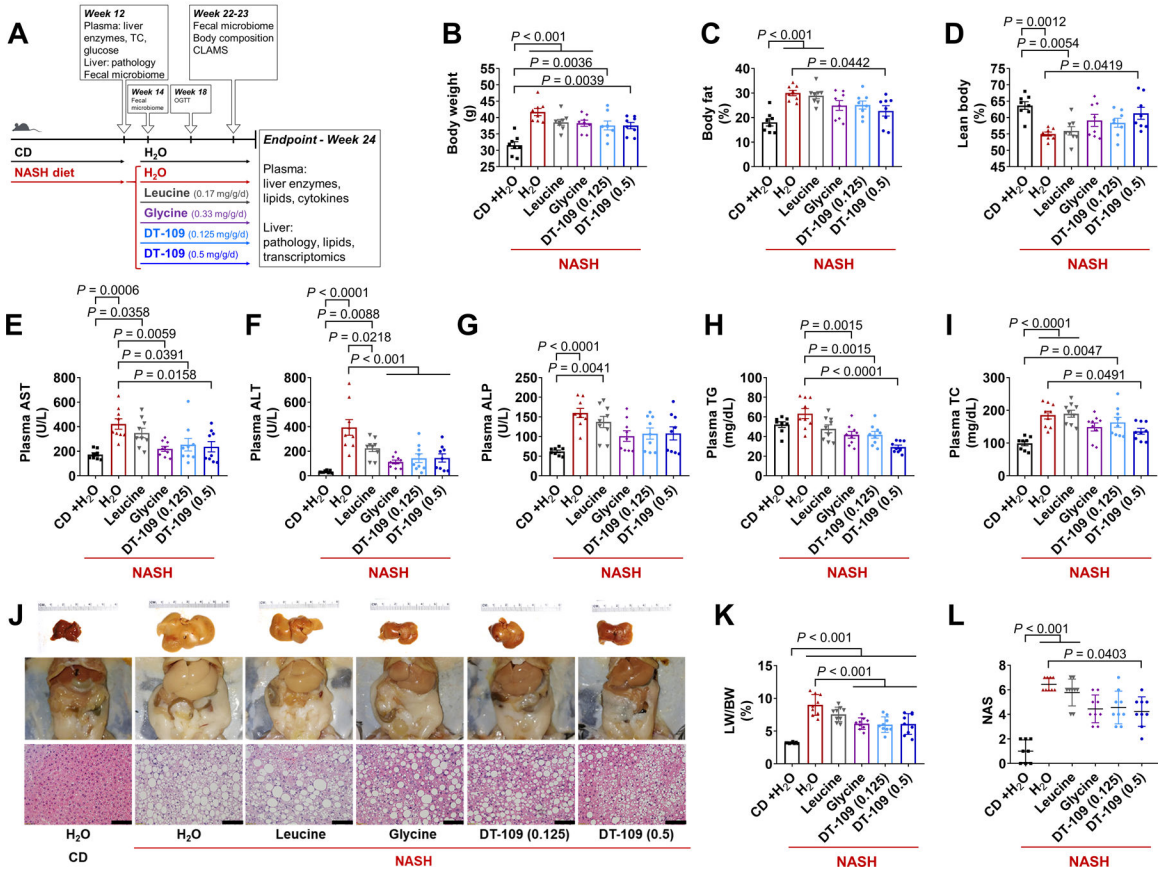

Fig. 4. DT-109 protects against diet-induced NASH.

(A) C57BL/6J mice were fed CD or NASH-diet for 12 weeks. After NASH confirmation, mice were randomized to receive 0.125 or 0.5 mg/g/day DT-109 or equivalent amounts of leucine, glycine (0.17, 0.33 mg/g/day) or H_2O via oral gavage for an additional 12 weeks on NASH-diet. Mice fed CD and administered H_2O served as control (n=8–9). NMR-based body composition analysis at weeks 22–23: **(B)** Body weight, **(C)** fat (%), and **(D)** lean mass (%). Endpoint plasma analysis: **(E)** AST, **(F)** ALT, **(G)** ALP, **(H)** TG and **(I)** TC. **(J)** Gross morphology and H&E histology (Scale bar: 50 μm). **(K)** LW/BW ratio. **(L)** NAS. Data are means ± SEM. Statistical differences were compared by one-way ANOVA followed by Bonferroni post-hoc test or by Kruskal-Wallis test followed by Dunn's post-hoc test.

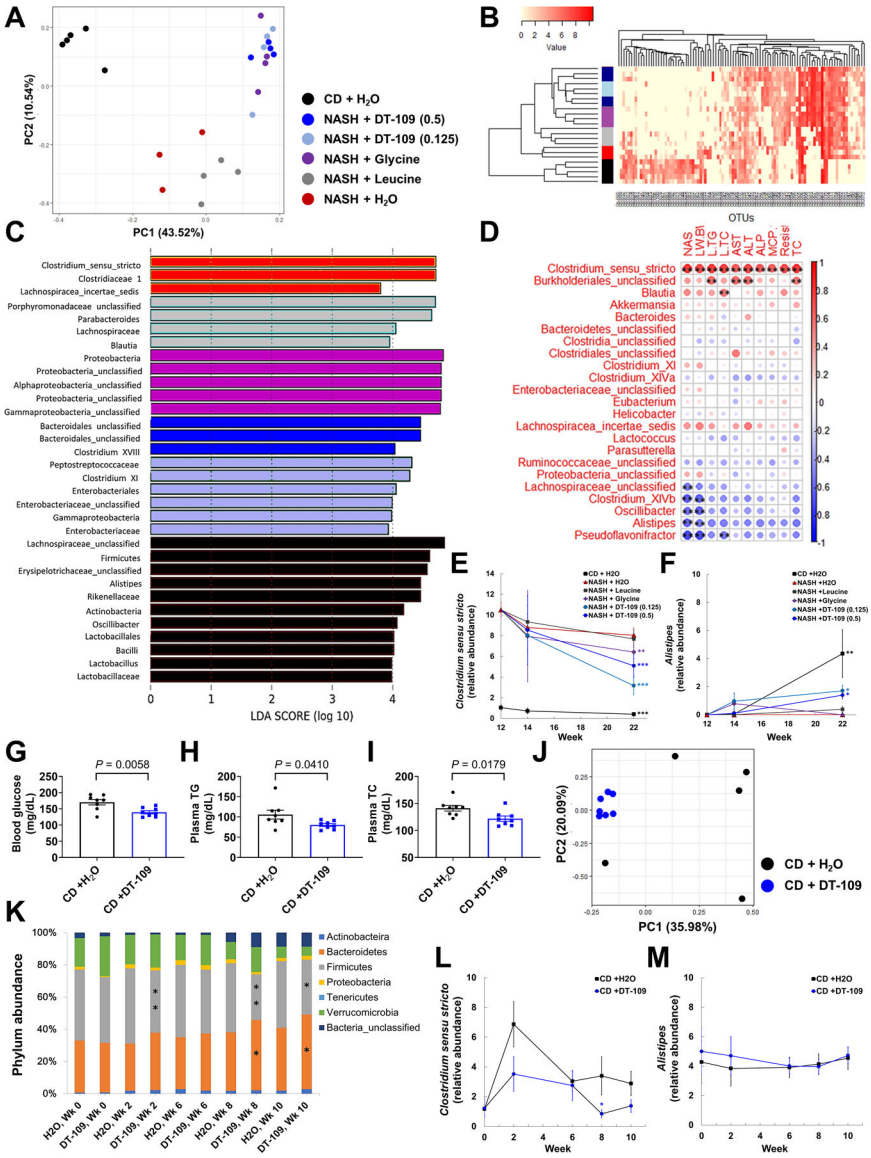

Fig. 5. The effects of DT-109 on the gut microbiome on NASH-diet and CD.

Fecal samples were obtained after 10 weeks of treatment on NASH-diet or CD (Fig. 4A). **(A)** PCA, **(B)** hierarchical clustering of OTUs in each group (sidebar colors as in A), **(C)** LDA of overrepresented bacterial taxa in each group, **(D)** correlations between altered genera and NAFLD-related parameters. Spearman's correlation coefficients are represented by color ranging from blue (−1) to red (+1), **P<0.01. Relative abundance of **(E)** *Clostridium sensu stricto* and **(F)** *Alistipes* in fecal samples from each group before (week 12), after 2 and 10 weeks of treatments. (n=3–5 cages) **P<0.01, ***P<0.001 vs. NASH before treatments. C57BL/6J mice were fed CD and treated with 0.5 mg/g/day DT-109 for 10 weeks. **(G)** Endpoint non-fasting blood glucose, **(H)** plasma **TG** and **(I)** TC (n=8 mice). Fecal samples were obtained at baseline and after 2, 6, 8 and 10 weeks of DT-109 treatment: **(J)** PCA at endpoint, **(K)** phylum-level comparison, **(L)** *Clostridium sensu stricto* and **(M)** *Alistipes* in fecal samples from each group throughout the study (n=5–7 cages), *P<0.05,

**P<0.01 vs. CD +H_2O. Data are means ± SEM. Statistical differences were compared using Student's t test or Mann-Whitney U test or using one-way ANOVA followed by Bonferroni post-hoc test or by Kruskal-Wallis test followed by Dunn's post-hoc test.

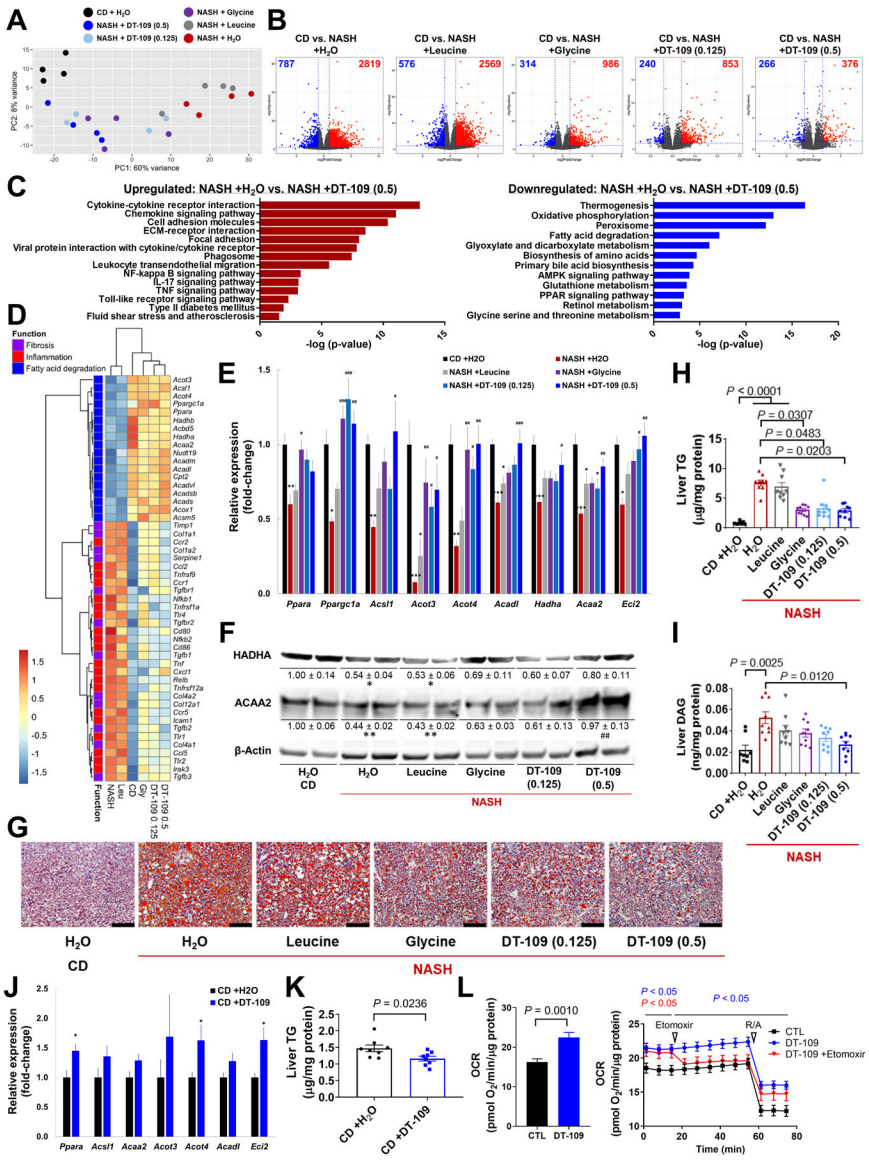

Fig. 6. Glycine-based treatment corrects impaired FAO, HS, and lipotoxicity induced by NASH-diet.

RNA-sequencing of livers collected at endpoint (n=4): **(A)** PCA, **(B)** volcano plots of DEG in each group compared to CD (blue: downregulated; Red: upregulated), **(C)** pathway analysis comparing NASH+H_2O to NASH+0.5 mg/g/day DT-109. Pathways enriched in the up- or downregulated DEG are plotted in red or blue, respectively, **(D)** heatmap of NASH-related DEG across all experimental groups (log2fold-change vs. CD). **(E)** qPCR validation of FAO-related DEG in independent samples (n=8), *P<0.05, **P<0.01, ***P<0.001 vs. CD; $^{\#}$P<0.05, $^{\#\#}$P<0.01, $^{\#\#\#}$P<0.001 vs. NASH+H_2O, and **(F)** Western blot (n=4). **(G)** ORO histology (Scale bar: 100μm), **(H)** liver TG and **(I)** DAG (n=8–9). C57BL/6J mice were fed CD and treated with 0.5 mg/g/day DT-109 for 10 weeks (n=8). **(J)** qPCR analysis of FAO-related genes relative to *Gapdh*. **(K)** Liver TG. **(L)** HepG2 cells were treated with or without 1 mM DT-109 for 24 h followed by Seahorse analysis of OCR in the absence or presence of 6 μM etomoxir (n=3). Data are means ± SEM. Statistical differences were compared using

Student's t test or Mann-Whitney U test or using one-way ANOVA followed by Bonferroni post-hoc test or by Kruskal-Wallis test followed by Dunn's post-hoc test. Significance of the enriched pathways was determined by right-tailed Fisher's exact test followed by Benjamini-Hochberg multiple testing adjustment.

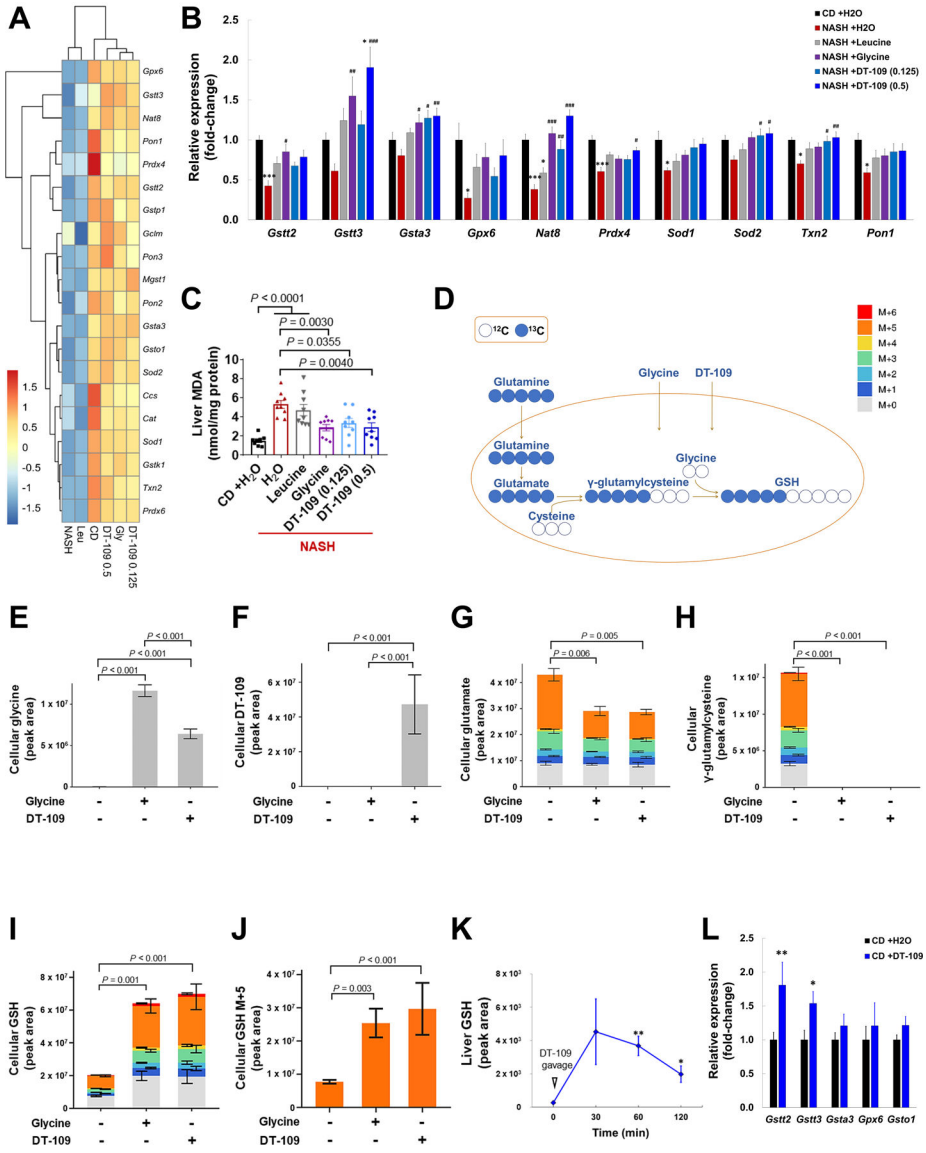

Fig. 7. Antioxidant effects of glycine-based treatment via *de novo* GSH synthesis.

(A) Heatmap of redox-related DEG across all experimental groups (log2fold-change vs. CD, n=4). **(B)** qPCR validation of related genes in independent samples (n=8). *P<0.05, ***P<0.001 vs. CD; #P<0.05, ##P<0.01, ###P<0.001 vs. NASH+H_2O. **(C)** Liver MDA (n=8–9). **(D)** Schematic representation of labeling *de novo* synthesized GSH from $^{13}C_5$-labeled glutamine, cysteine and glycine. AML-12 cells were cultured with 1 mM $^{13}C_5$-labeled glutamine for 5 h in the presence or absence of glycine or DT-109 (1 mM). Isotopologue distribution (normalized peak area) of indicated cellular metabolites as determined by LC-MS (n=2–4): **(E)** Glycine, **(F)** DT-109, **(G)** glutamate, **(H)** γ-glutamylcysteine, **(I)** GSH and **(J)** M+5 isotopologue of GSH. **(K)** LC-MS analysis of liver GSH before and after 30, 60 and 120 min from oral administration of 0.5 mg/g DT-109 to C57BL/6J mice (n=3). **(L)** Mice were fed CD and treated with 0.5 mg/g/day DT-109 for 10 weeks. Liver expression of genes regulating GSH metabolism relative to *Gapdh* by qPCR (n=8). Statistical differences

were compared using Student's t test or Mann-Whitney U test or using one-way ANOVA followed by Bonferroni post-hoc test or by Kruskal-Wallis test followed by Dunn's post-hoc test.

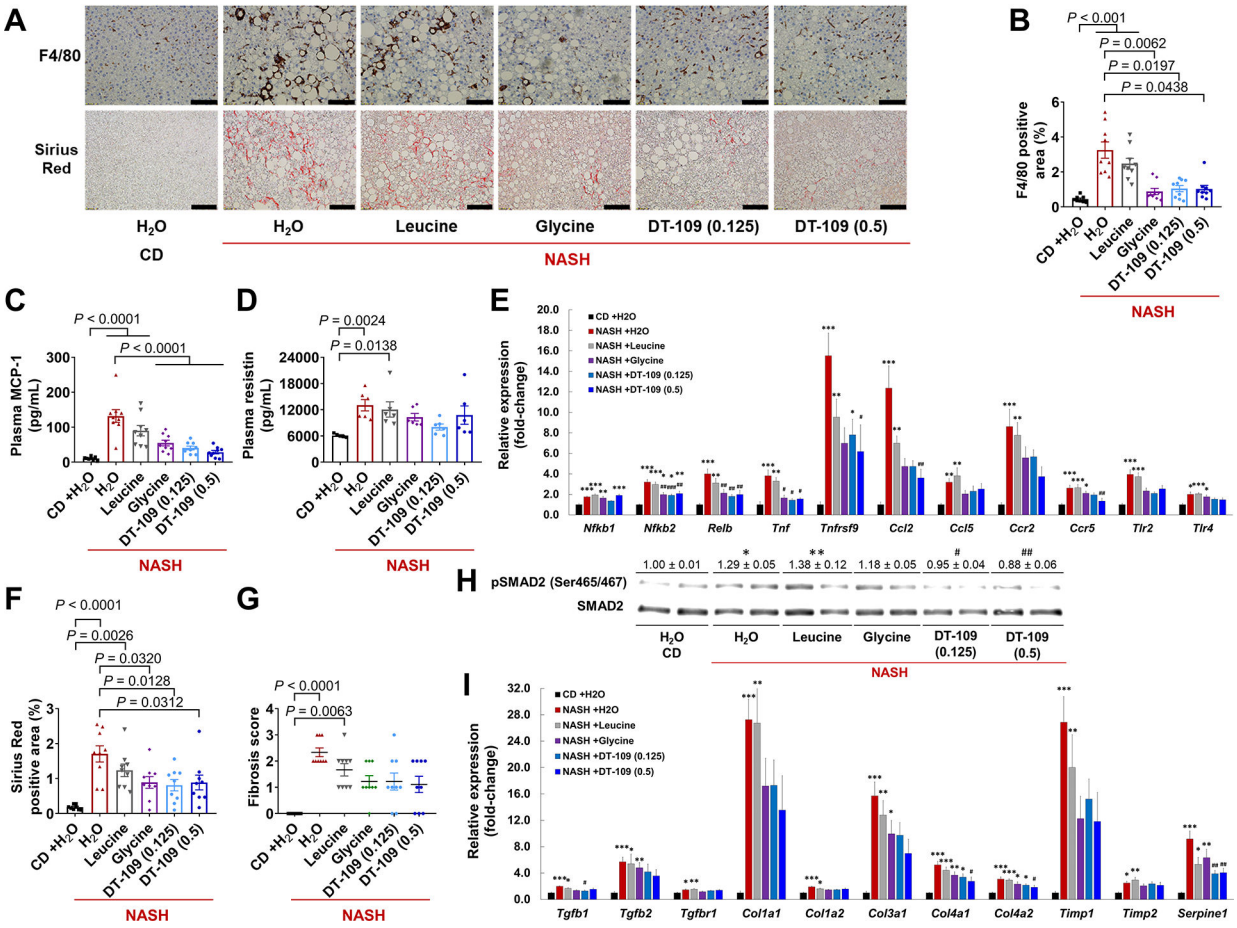

Fig. 8. Glycine-based treatment reduces hepatic inflammation and fibrosis induced by NASH-diet.

(A) F4/80 immunohistochemistry and Sirius Red histology (Scale bar: 50 μm), **(B)** F4/80 positive area (n=8–9). **(C)** Plasma MCP-1 (n=8–9), and **(D)** resistin (n=5–6). **(E)** qPCR validation of inflammation-related genes in independent samples (n=8). **(F)** Sirius Red positive area. **(G)** Fibrosis score. **(H)** Western blot of phosphorylated-SMAD2 (Ser465/467) and total-SMAD2. **(I)** qPCR validation of fibrosis-related DEG. *P<0.05, **P<0.01, ***P<0.001 vs. CD; $^{\#}$P<0.05, $^{\#\#}$P<0.01, $^{\#\#\#}$P<0.001 vs. NASH+H_2O. Data are means ± SEM. Statistical differences were compared by one-way ANOVA followed by Bonferroni post-hoc test or by Kruskal-Wallis test followed by Dunn's post-hoc test.